Fermilab

Managed by Fermi Research Alliance, LLC for the U.S. Department of Energy Office of Science

Low Level RF Control System

Brian Chase

PIP-II Machine Advisory Committee Meeting

10-12 April 2017

Outline

- LLRF system overview and requirements
- Simulation and Results
- Project Status
- RF Interlocks Overview

LLRF System Overview

LLRF Scope and requirements

- RF field control of all Linac Cavities capable of pulsed and CW operation
  - Individual cavities regulated to 0.01%, 0.01 deg. rms
- multi-frequency Master Oscillator and Phase Reference lines
- Beam Chopper Waveform Generator
  - RF locking source for Booster during beam fill
  - Timing source
- Resonance control hardware

LLRF Systems needed to meet R&D Goals

- 325 MHz Horizontal test stand
  - Support for CW and pulsed mode (Operational)
- 650 MHz Horizontal test stands
  - Support for CW and pulsed mode operation(To be supplied by India)
- PIP2-IT
  - Master Oscillator and Phase Reference distribution line
    - 162.5 MHz & 325 MHz (Operational)
  - RFQ – 162.5 MHz (Q4FY15)
    - 2 RF amplifier system (Operational in pulsed and CW modes)
  - Buncher - 3 cavities - 162.5 MHz (1st buncher operational)
  - Half Wave Resonators - 8 cavities @162.5 MHz
  - SSR1 - 8 cavities @ 325 MHz
  - Kicker waveform generator

LLRF System Approach

Table 3.23: Parameters of RF amplifiers

	Frequency (MHz)	Number of RF cavities	Number of RF amplifiers per cavity	Regime of operation	RF amplifier power (kW)	# 4 Cavity LLRF Stations
RFQ	162.5	1	2	CW	75	1
MEBT Bunching cavities	162.5	4	1	CW	3	1
First HWR cavity	162.5	1	1	CW	3	2
Other HWR cavities	162.5	7	1	CW	7	4
SSR1	325	16	1	Pulsed	7	9
SSR2	325	35	1	Pulsed	20	
LB650	650	33	1	Pulsed	40	15
HB650	650	24	1	Pulsed	70	

- LLRF hardware is compatible for all frequencies and is repeated in racks controlling four cavities
- Each cavity frequency has its own phase reference and LO
- All systems have a common IF (20 MHz)
- Low noise and crosstalk, high linearity

Synergy Between LLRF DOE Projects at FNAL

	RF Converters	Digital controller	Algorithms FW/SW	Phase Reference Line	Resonance Control
NML-ILC	FNAL v1,v2	FNAL MFC	FNAL v1	FNAL v1	Development
PIP2 IT HTS	v3	SOC-MFC	FNAL ongoing	in development	
CMTS-1	v3	SOC-MFC	FNAL ongoing	simplified	
LCLS-II 1.3 GHz	FNAL v4	LBNL	LBNL	SLAC/FNAL	JLAB/FNAL
PIP2 IIFC HTS1, HTS2	v5	SOC and LCLS-II	Based on FNAL and LCLS-II	New design based off of NML	Based on our LCLS-II work
Mu2e G-2		SOC-MFC			

PIP2-IT RF Stations Diagram

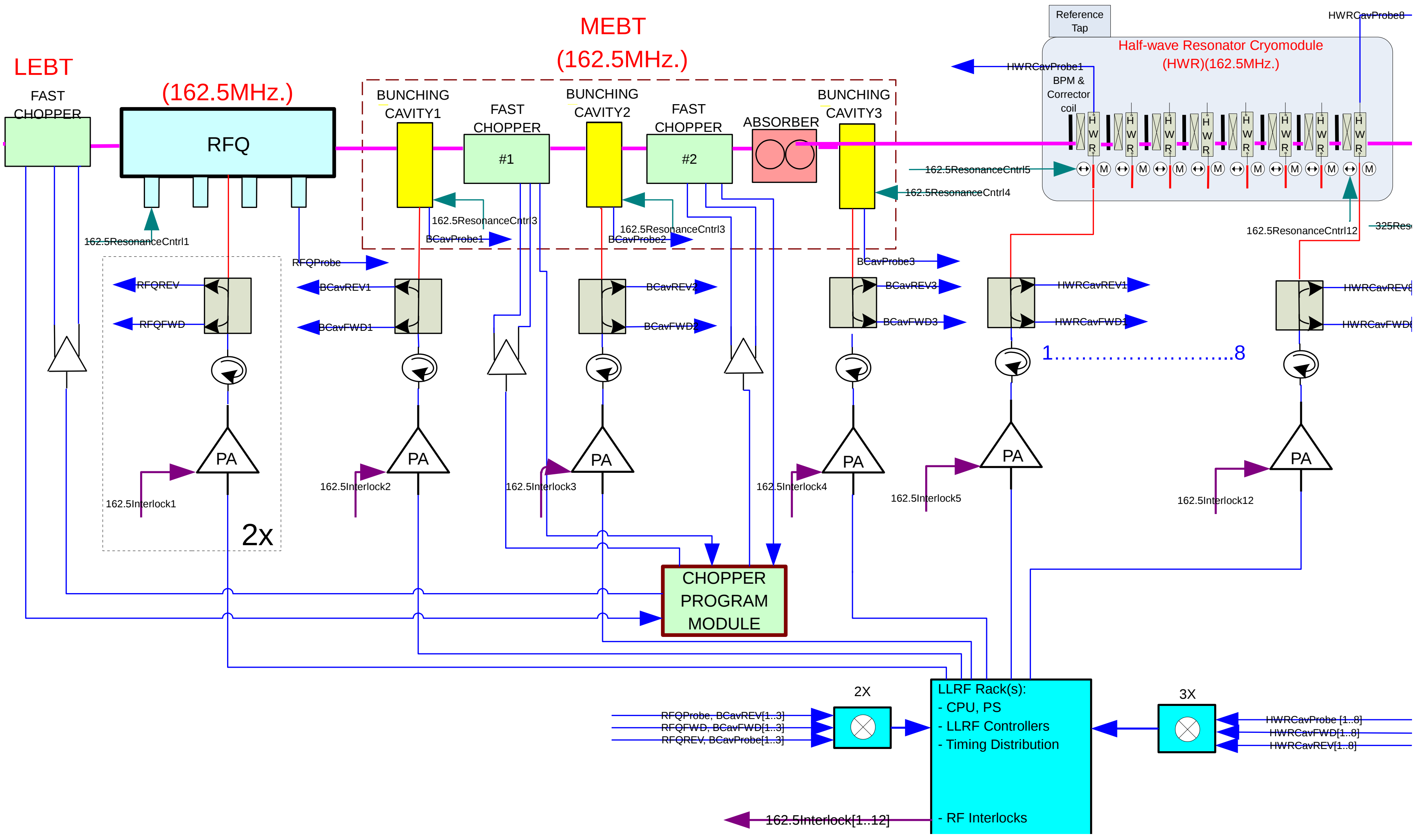

Fermilab PIP-II

Basic LLRF Station Diagram for 4 cavities

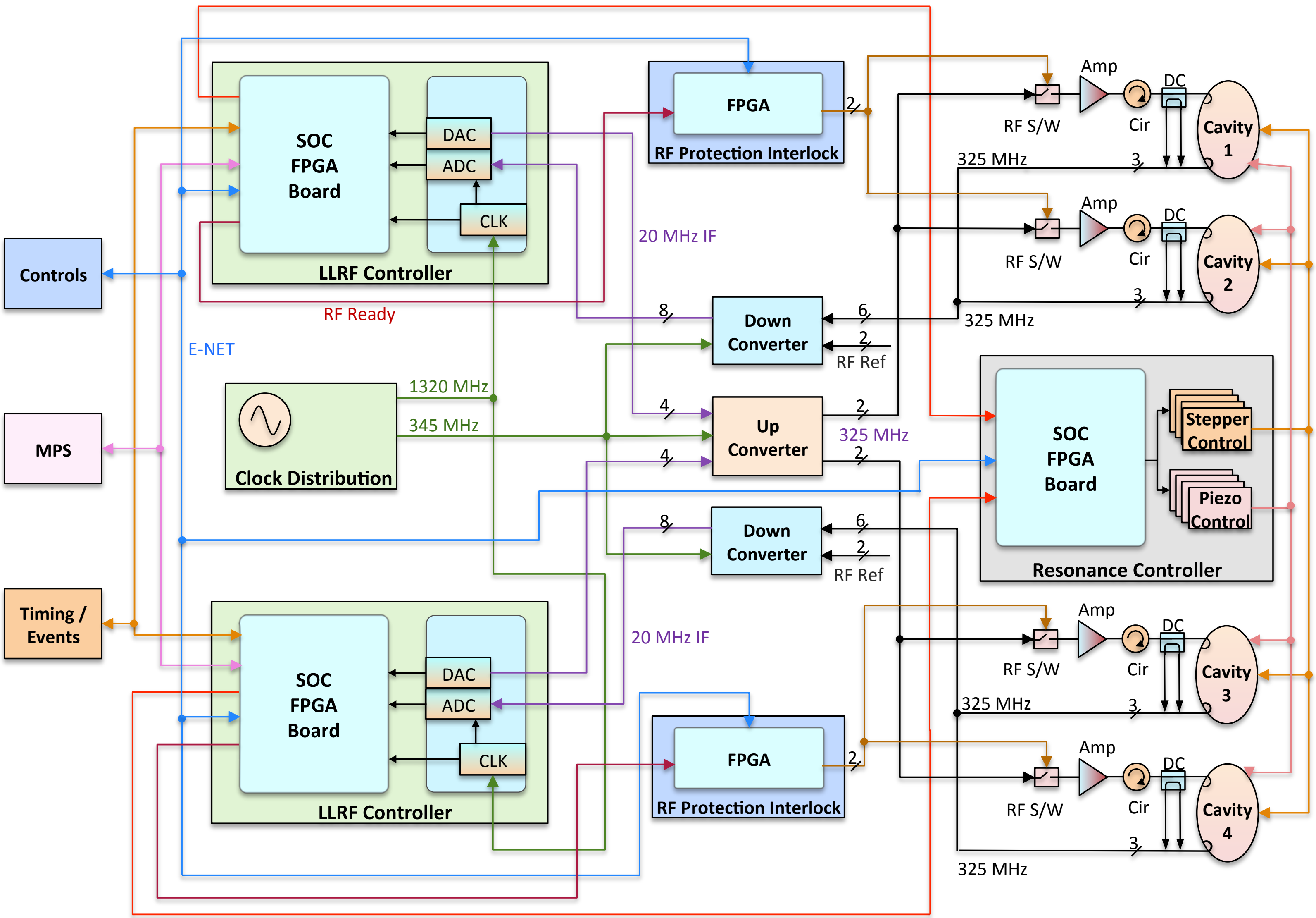

Fermilab PIP-II

PIP-II LLRF rack layout - front and rear view

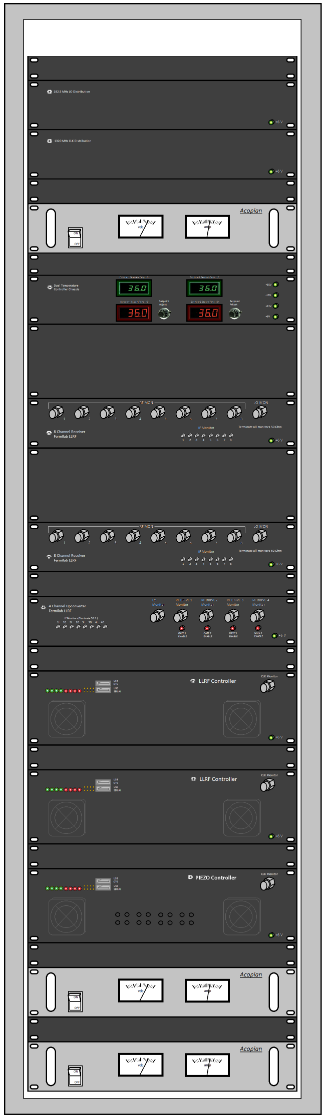

182.5 MHZ LO DISTIBUTION

1320 MHZ CLK DISTIBUTION

RF POWER SUPPLY

DOWNCONVERTER TEMPERATURE CONTROL

8-CHANNEL DOWNCONVERTER

8-CHANNEL DOWNCONVERTER

4-CHANNEL UPCONVERTER

LLRF CONTROLLER

LLRF CONTROLLER

PIEZO CONTROLLER

PIEZO POWER SUPPLY

LLRF CONTROLLER POWER SUPPLY

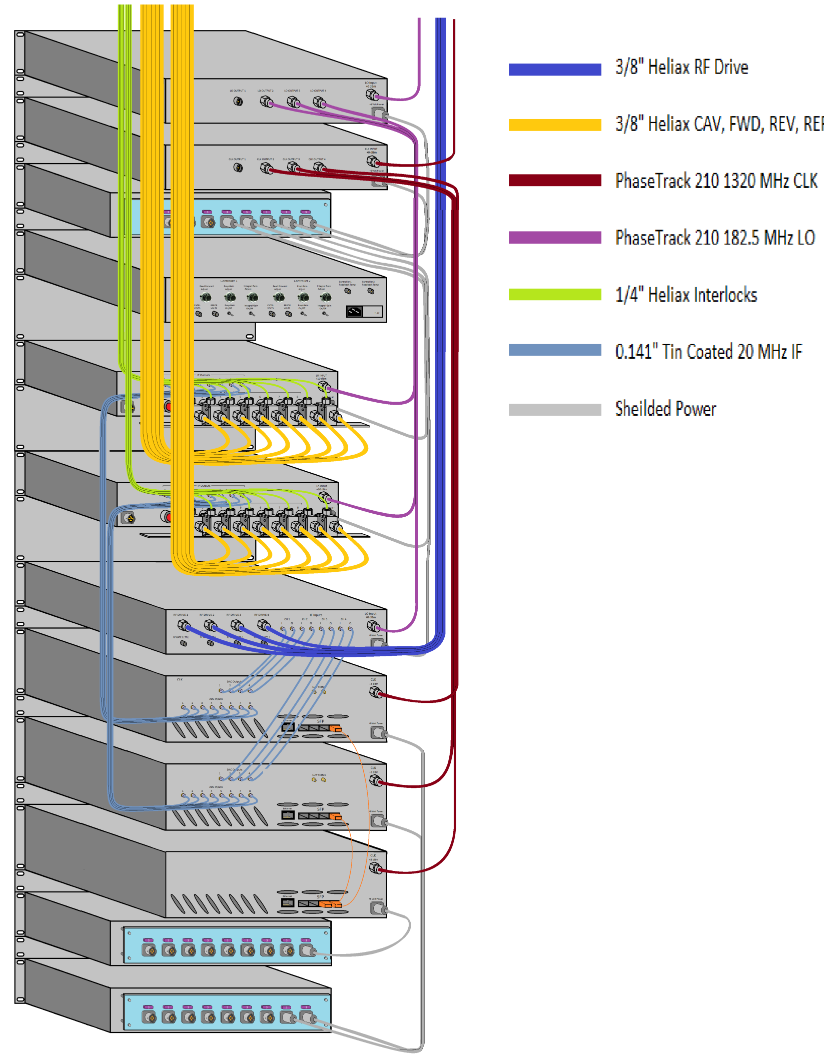

Fermilab PIP-II

4-Channel Up-converter

- 20 MHz IF input -2 dBm max
- 162.5, 325, and 650 MHz Output, +11 dBm max
- 13 dB IF to RF Conversion Gain typ.
- Channel to Channel Isolation > 88 dB
- Spurious Signal Suppression > 80 dB
- High isolation (>68 dB) TTL RF switch
- Power Supply 6V, 1.8 Amp

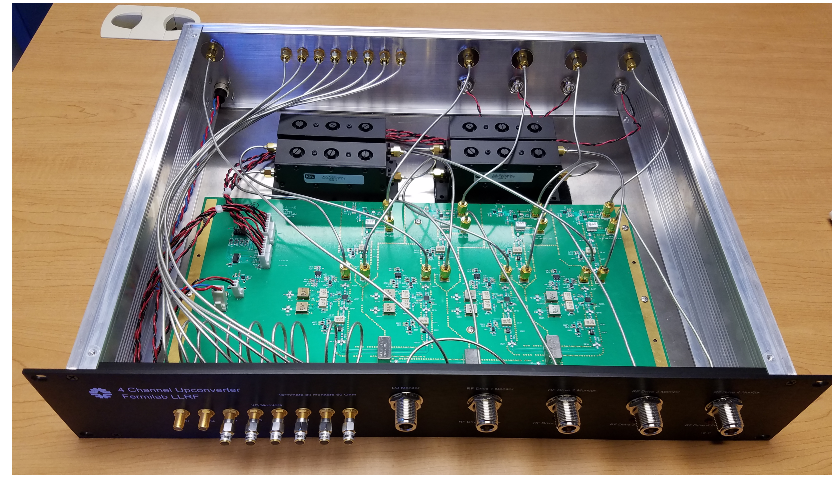

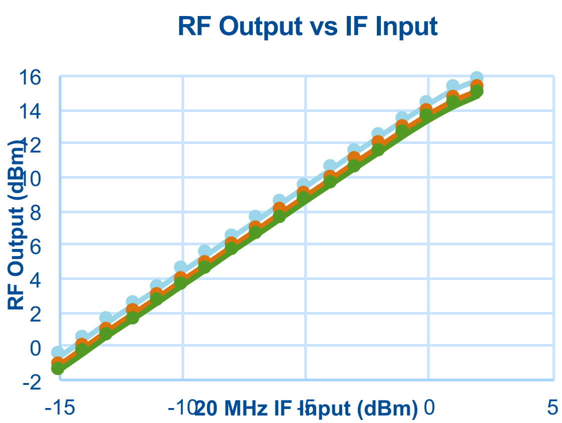

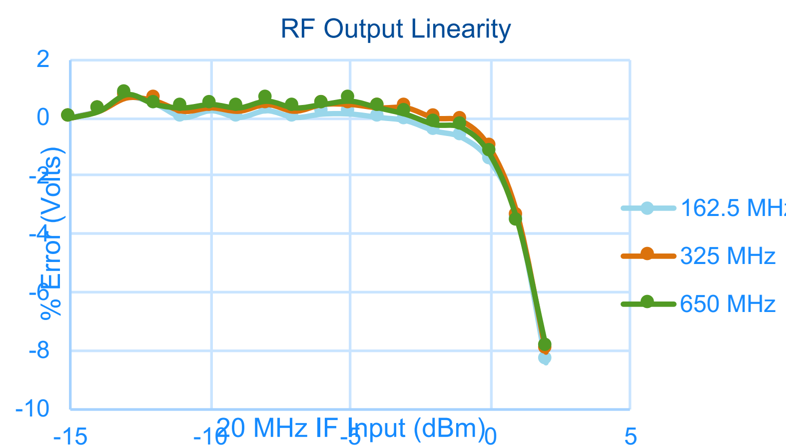

PIP-II LLRF 8-Channel Downconverter Prototype

- RF input 162.5 MHz – 650 MHz
- Less than 1% non-linearity up to 10 dBm RF input
- 1.8, 2.1, 2 dB conversion loss @ 162.5, 325, 650 MHz respectively
- Better than 82 dB Channel to Channel Isolation
- RF, LO, IF monitor ports
- Absorptive IF output low pass filter
- Noise output floor of -161 dBc/sqrt(Hz)
- Integrated output 1/f noise < 1.84 fsec, (0.02 to 20 Hz)
- LO Input power of 3.1, 3.8, and 5.7 dBm @ 162.5, 325, 650 MHz re
- Power Supply 6V, 2.25 Amps

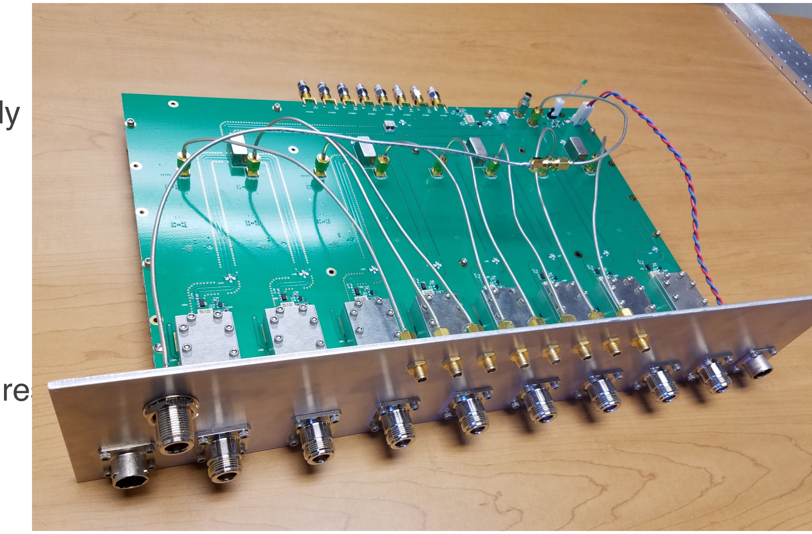

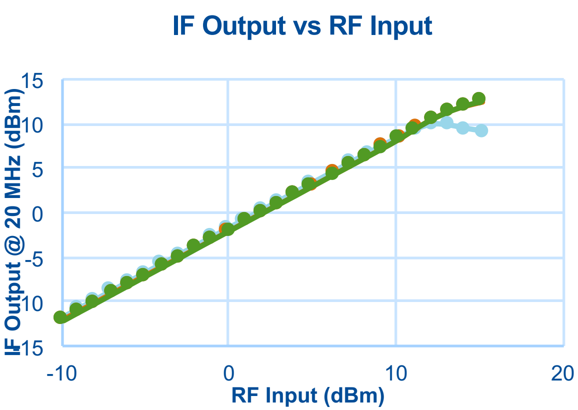

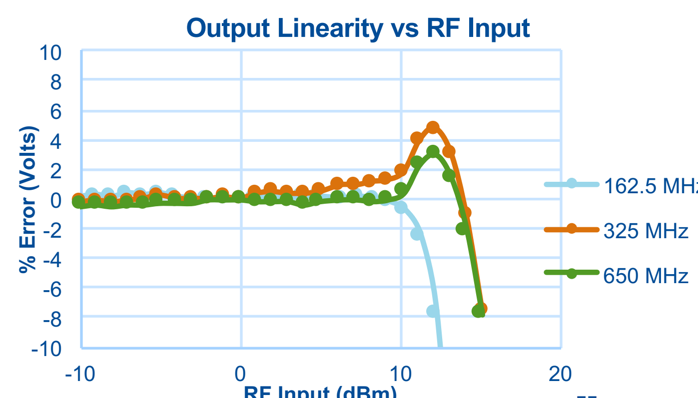

IIFC LLRF Status

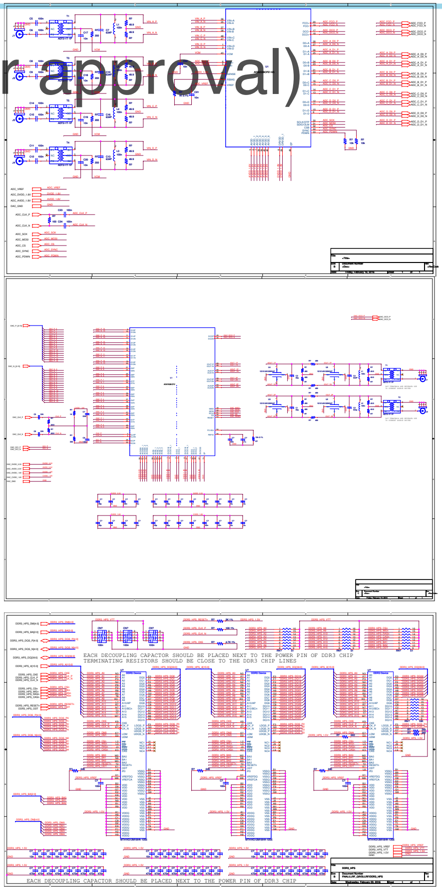

- Seven joint FRSs Approved (two more near approval)
  - TRS in process
- 8-Channel Down-Converters
  - BARC version is in manufacturing process
- 4-Channel Up-Converters
  - FNAL version tested
  - BARC version is in manufacturing process
- FPGA Board
  - In schematic review process
- ADC-DAC FMC Module
  - Ready for manufacturing
- Resonance Control Chassis
  - Leverage from FNAL LCLS-II design and is in progress

IIFC 8 Channel Down-converter

- Layout finalization for the 8 channel down-convertor is almost complete
- All components required to assemble the board and chassis are available at vendor site
- Procedure to assemble the board in the chassis has been tentatively finalised.
- Tentative delivery date at BARC: Last week of May 2017
- Performance results of the boards should be available by: Second week of June 2017

4 Channel Up-converter

- Tentative delivery date at BARC: Third week of April 2017
- Performance results of the board should be available second week of May 2017

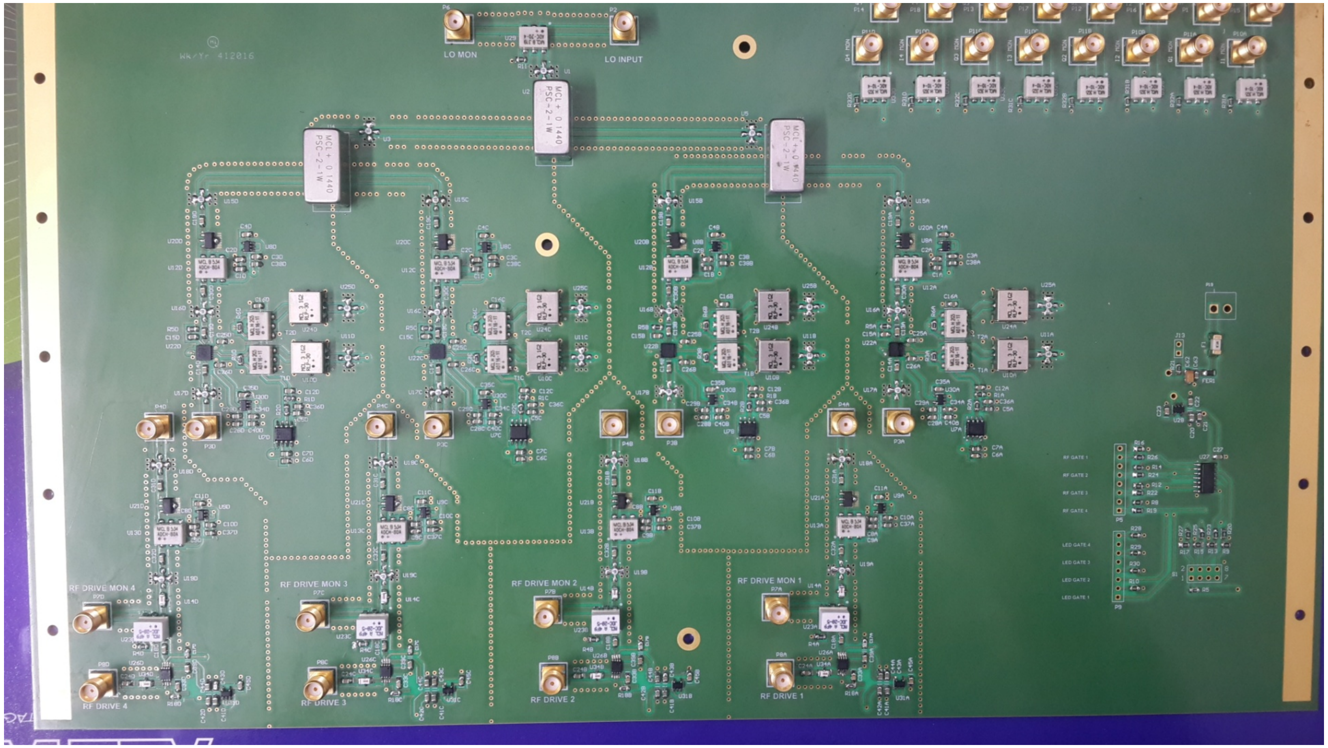

IIFC Designs

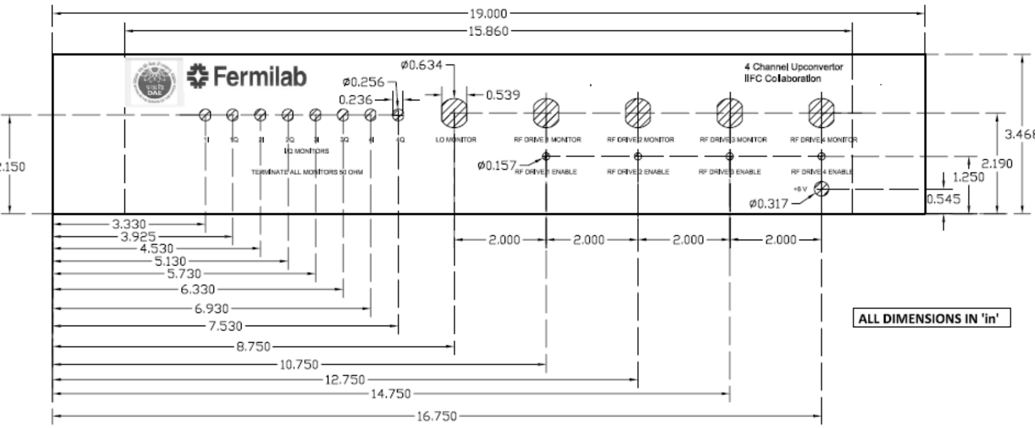

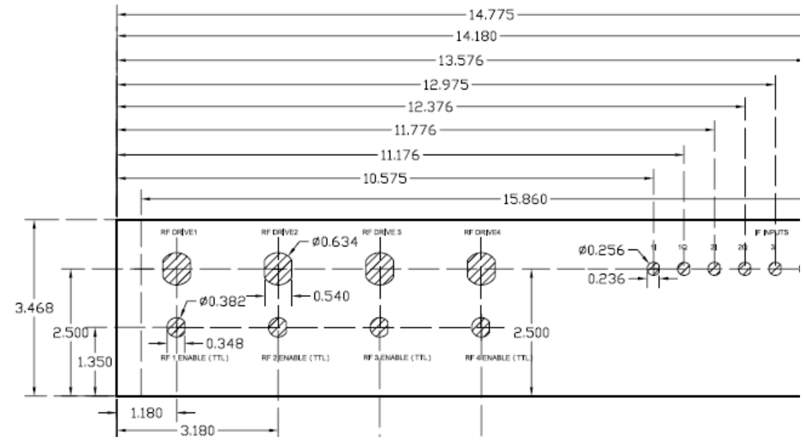

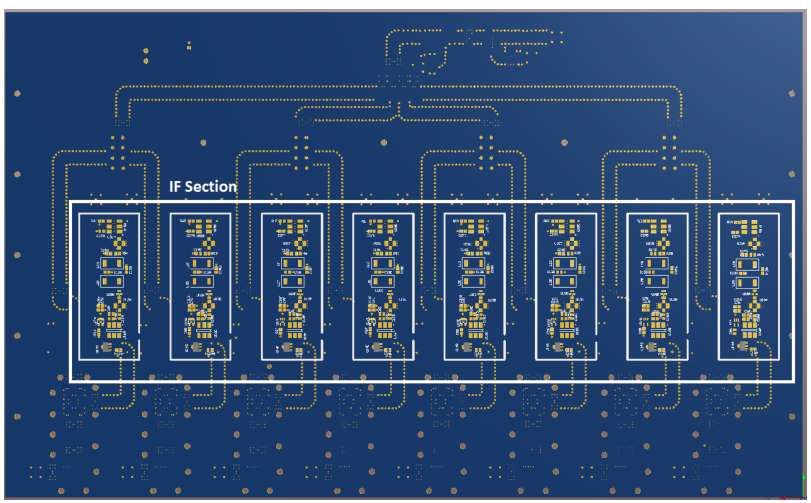

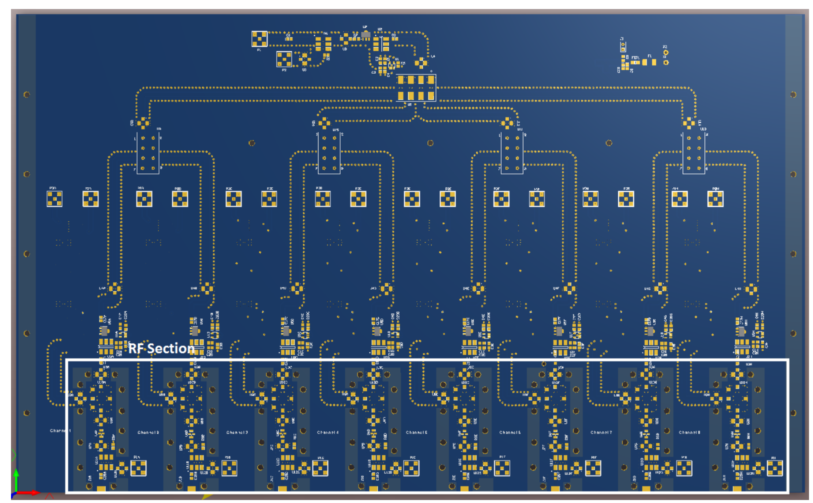

Fermilab PIP-II

Piezo Resonance Control Requirements

- Minimize microphonics and LFD to < 20 Hz
- 1 Hz or better resolution
- +- 1kHz tuning range
- 2 drive amplifiers for 2 piezo stack groups per cavity
  - (1 module per cavity)
  - 4 drive modules per chassis

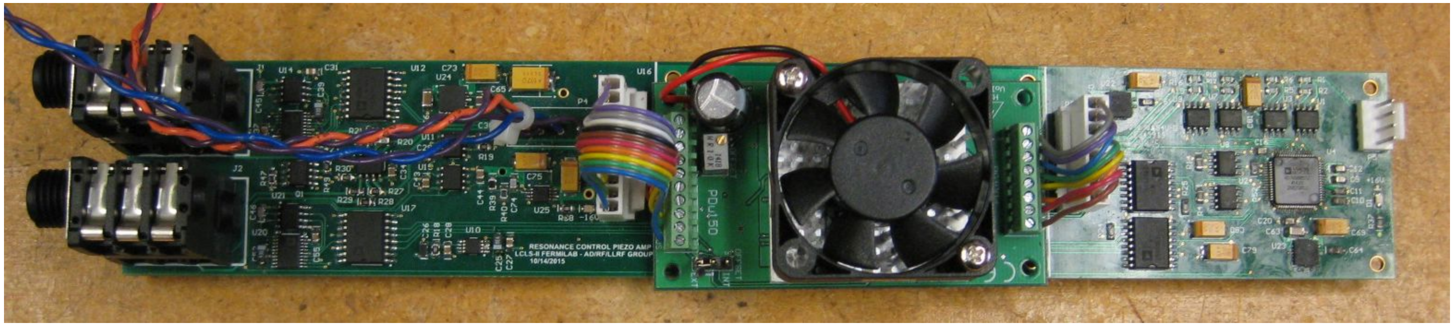

Resonance Control Chassis

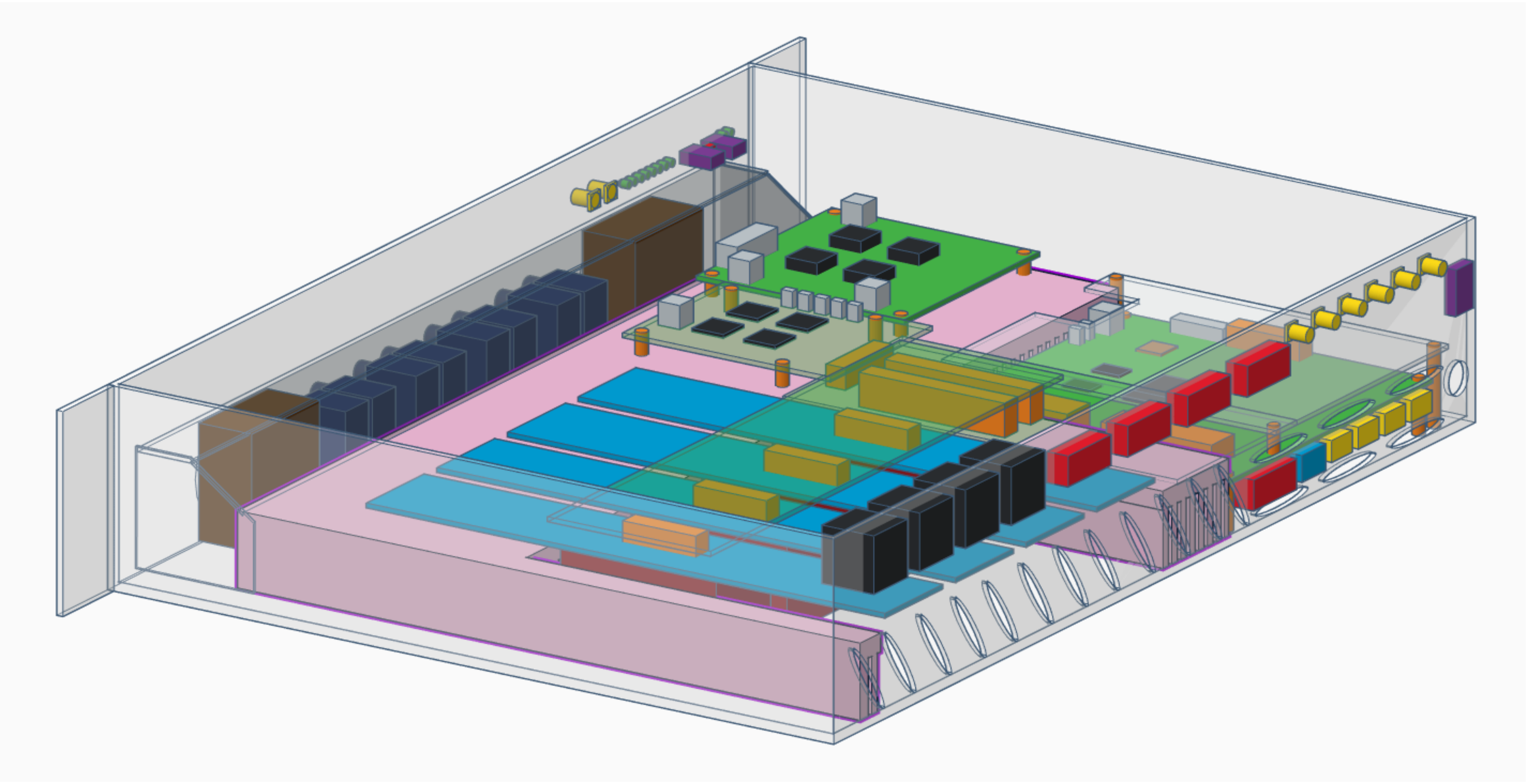

Fermilab PIP-II

Digitizer Chassis

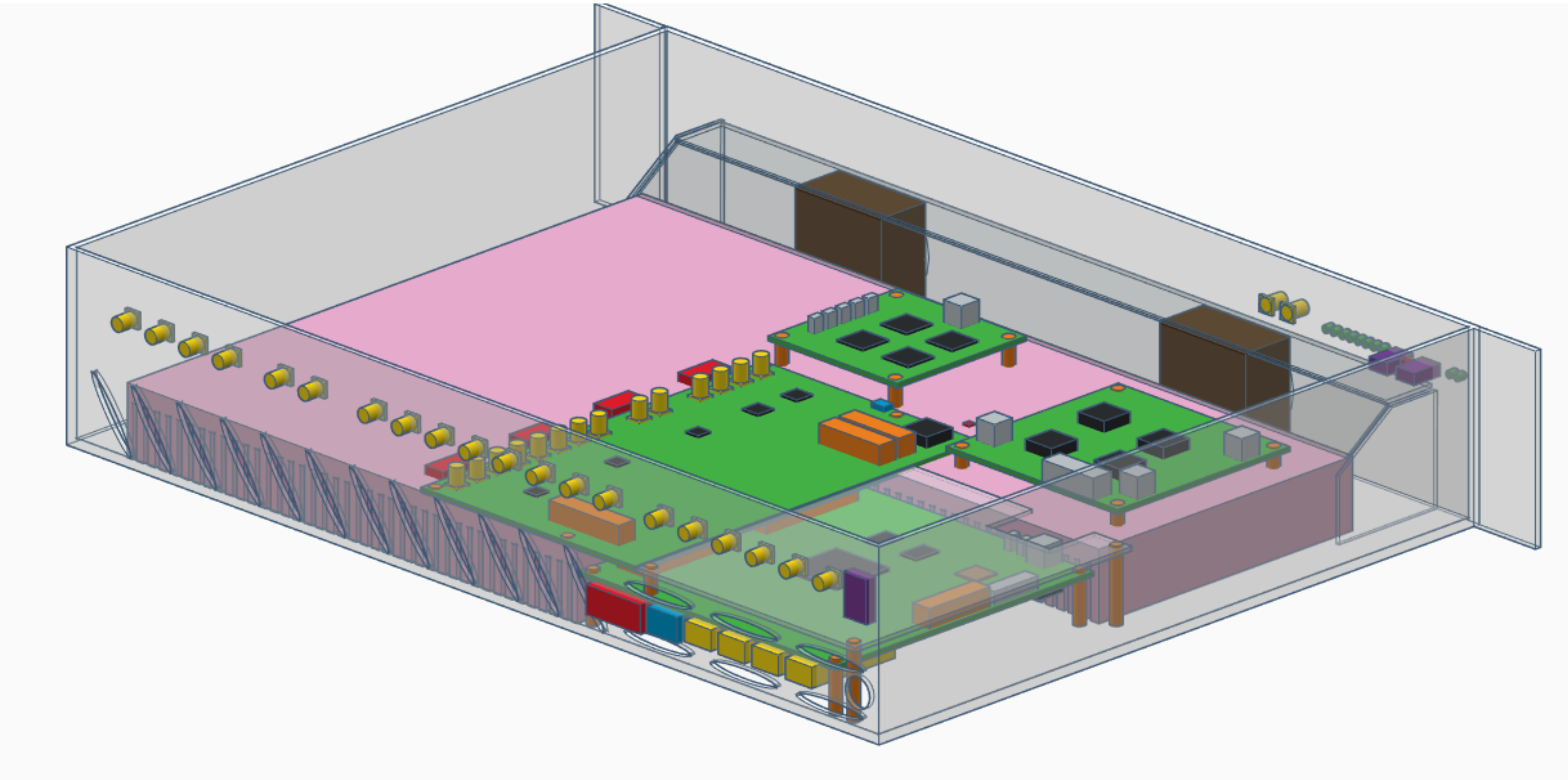

Phase Reference Lines (162.5, 325, 650 ,1300 MHz)

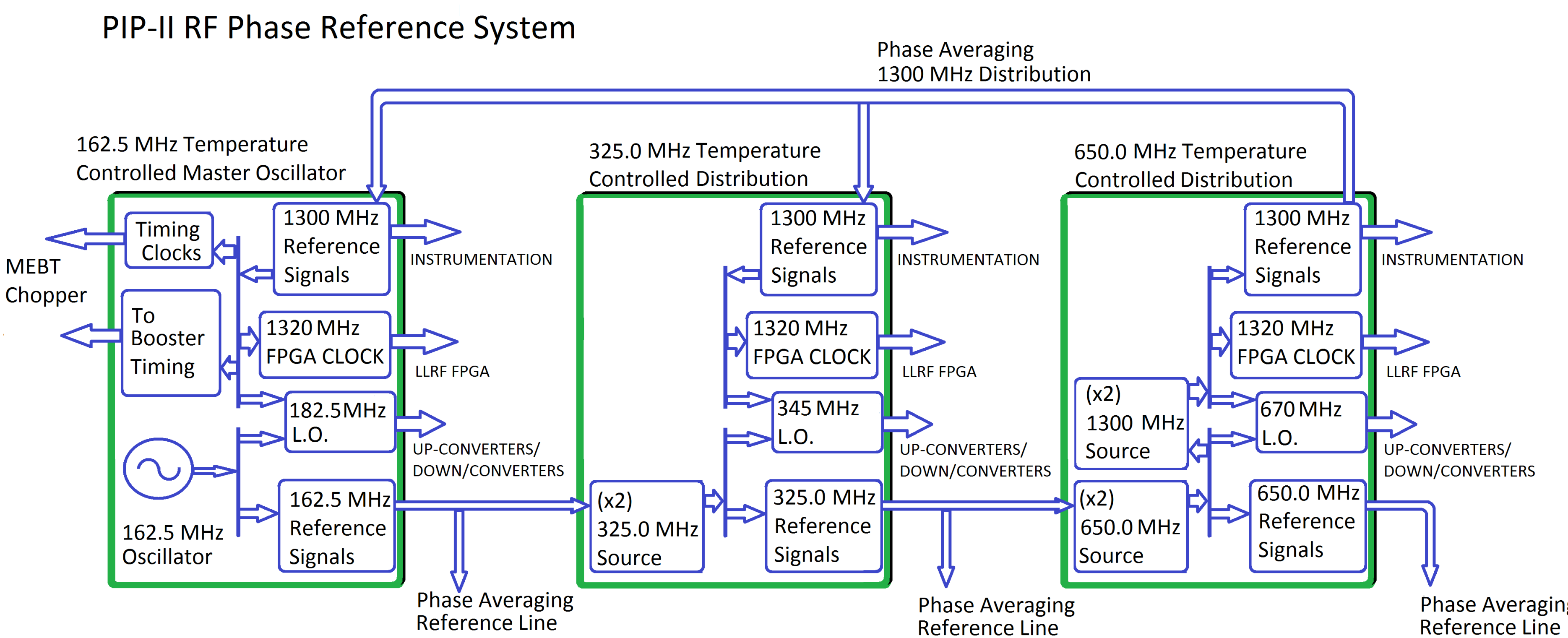

Multi-frequency Phase References and Local Oscillators Being prototyped at BARC

Details of First 162.5 MHz RF Section

Phase stability across harmonics (400 fs)

Temperature controlled racks and component plates

We have this experience and see a path forward

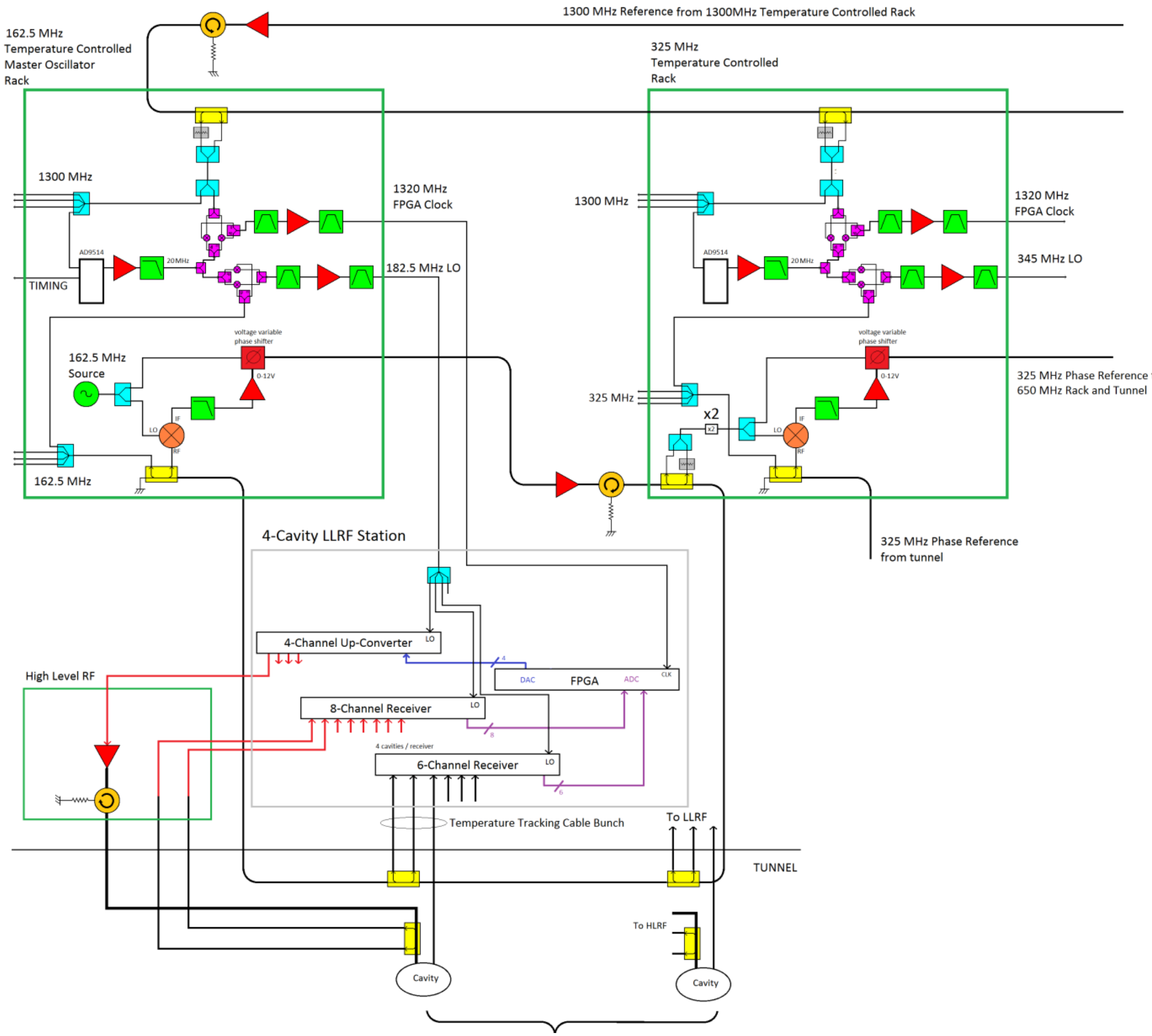

Fermilab PIP-II

Simulation and Results

Primary Technical Risks

- Resonance and Field Control for 5 new cavity designs
  - Lorentz Force Detuning compensation for narrow bandwidth cavities operated in pulsed mode
  - New cavity designs with new mechanical properties
  - 20 Hz power BW with expected 420 Hz Lorentz Force Detuning in SSR1
  - See resonance control talk
- 10^{-4} beam energy regulation with pulsed proton accelerator
  - Fill to flattop transient
  - Beam loading transient
  - RF system transient response

RF system control diagram

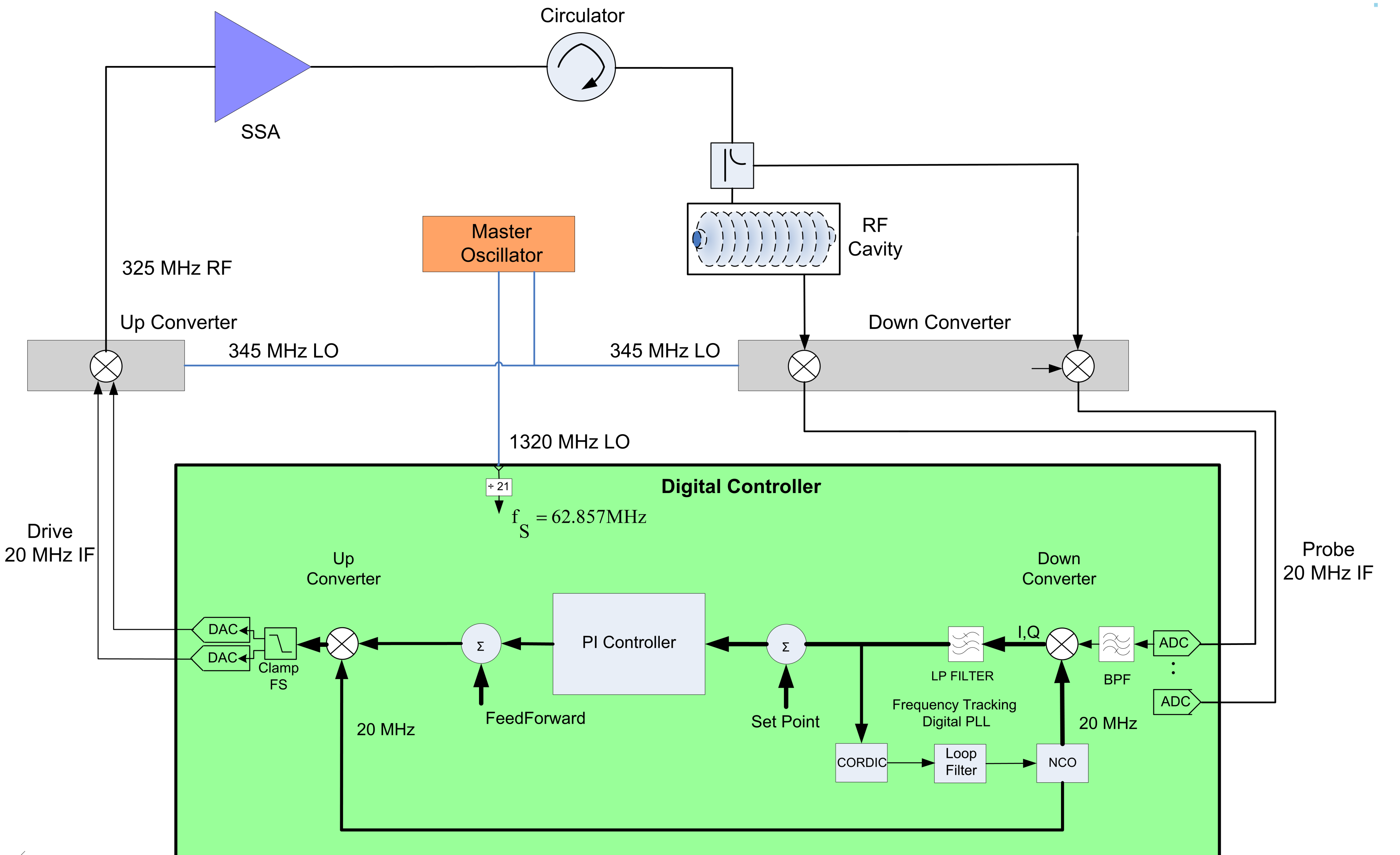

Fermilab PIP-II

Feedback requirements and analysis

- Expecting large disturbances from LFD, want fast response from beam loading transient
  - get 15 dB from feedforward beamloading compensation
- Approach - find highest stable loop gain and determine system noise requirements
- Determine best gain settings from operational experience and needs of beam-based feedback
  - It is easy to turn down the gain on a well designed system, impossible to turn up gain on a poorly designed one

- Assume a low noise oscillator
  - Wenzel VHF ULN 100 MHz 13.7 dBm
  - % http://www.wenzel.com/model/vhf-uln/
- System loop delay of 2.1 μsec
- Cavity bandwidth 30 Hz

Open loop transfer function of cavity and controller

Magnitude

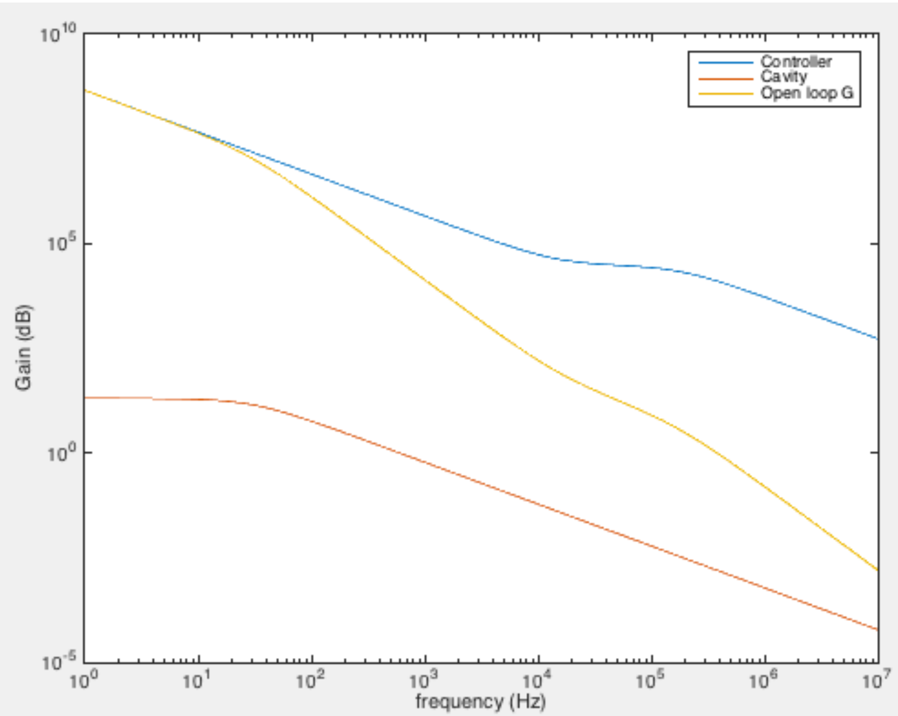

Phase

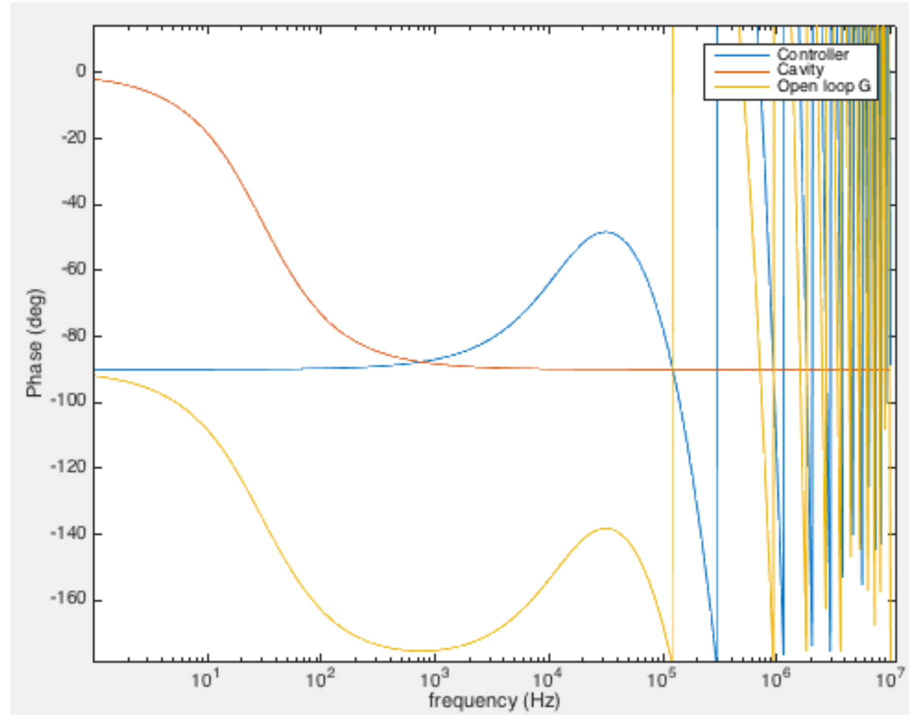

Max gain

Closed-loop bandwidth: ~50 kHz

Control system zero: 15 kHz

Proportional gain: 1500

Integral gain: 1.44e+08

Nominal gain

Closed-loop bandwidth: ~25 kHz

Proportional gain: 750

Integral gain: 7e+07

RFQ and Buncher pulsed response

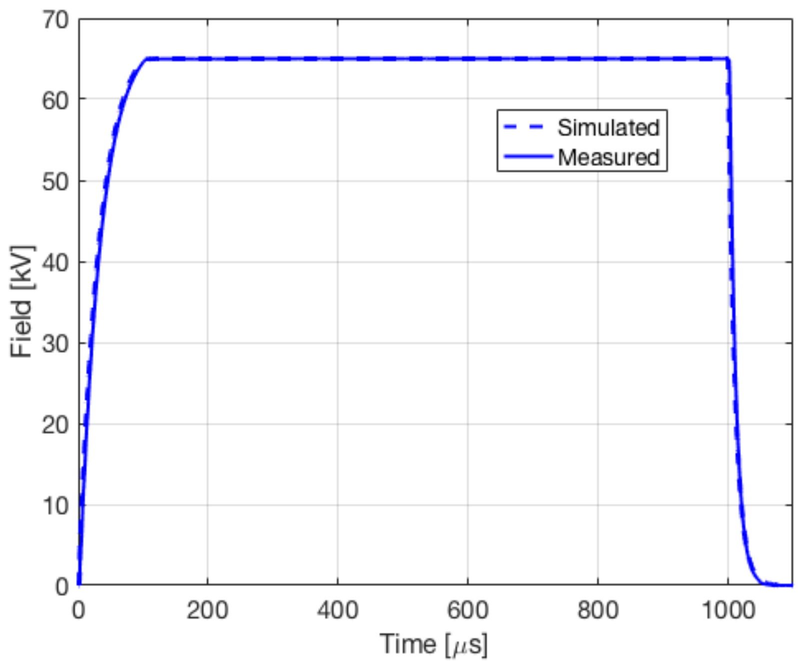

RFQ Pulse measured vs. simulated (Proportional and integral gains were 9.0 and 8.0e5 respectively)

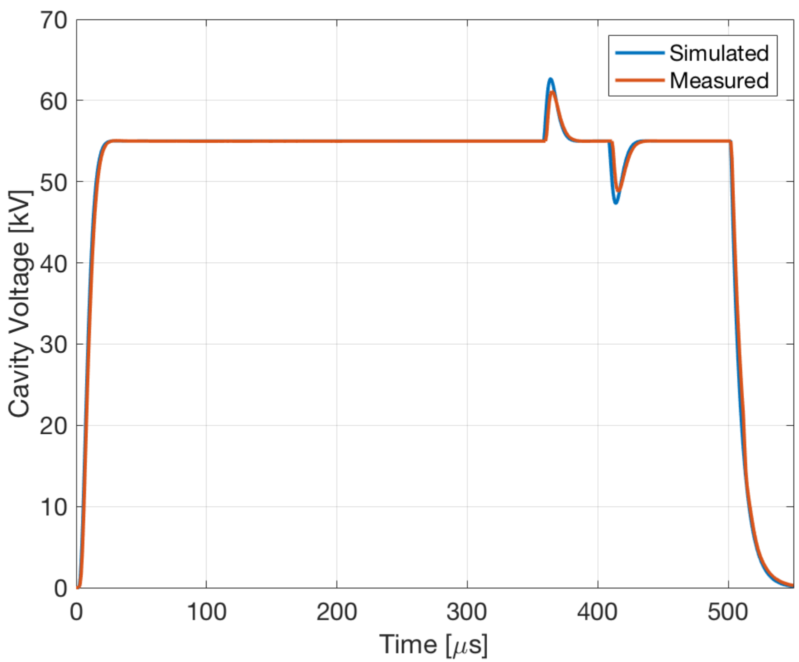

Buncher simulated vs. measured (kp 3.5, ki 6.0e5, Ql ~5000)

Fermilab PIP-II

Total phase noise to SSA from controller and oscillator

Closed loop response

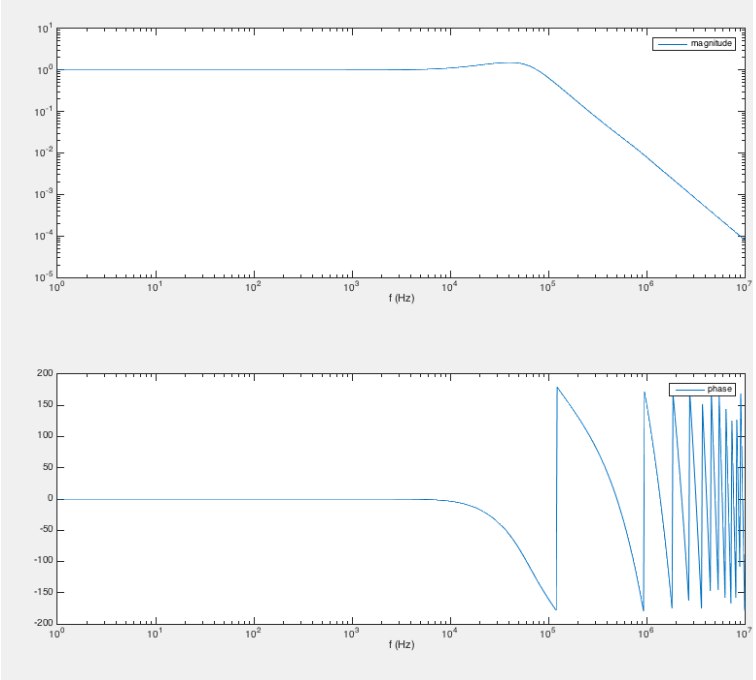

Cumulative SSA phase noise voltage

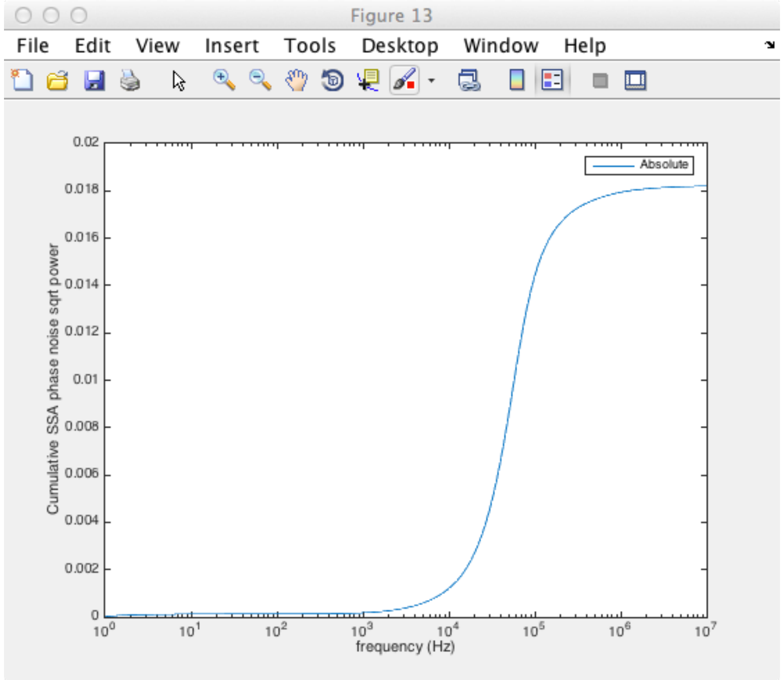

Careful attention to noise terms will allow high controller gains

- Cavity: 0.00078° rms
- SSA: 1.04°
- SSA from ADC noise 0.96°

Code developed for LCLS-II
Larry Doolittle LBNL and FNAL

Phase-energy Stability Simulations

- Studying the amplitude and phase regulation requirements and their impact on the LLRF system
  - Study effects of perturbations on the cavities through beam simulations
  - Develop code that performs basic beam dynamics calculations as well as RF feedback simulations to study the interaction between the RF system

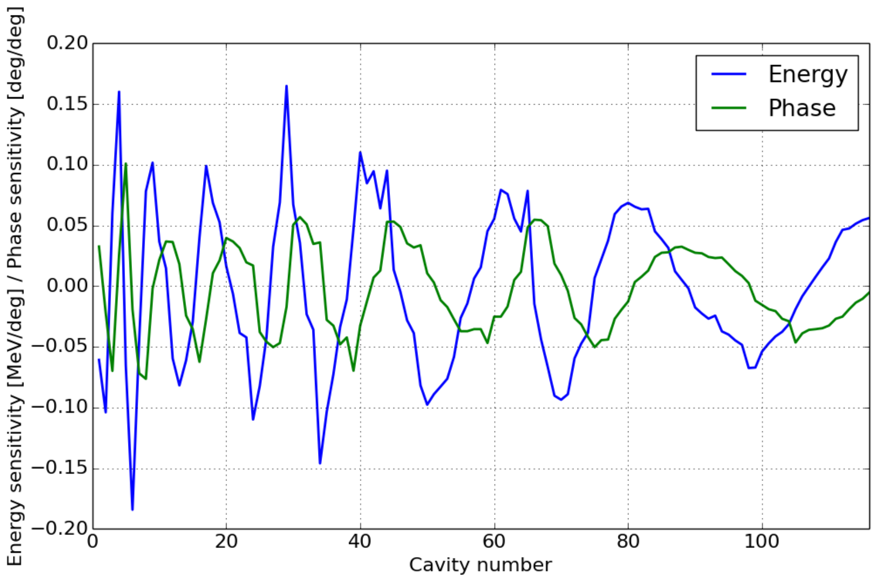

Linac output energy sensitivity to single cavity phase errors

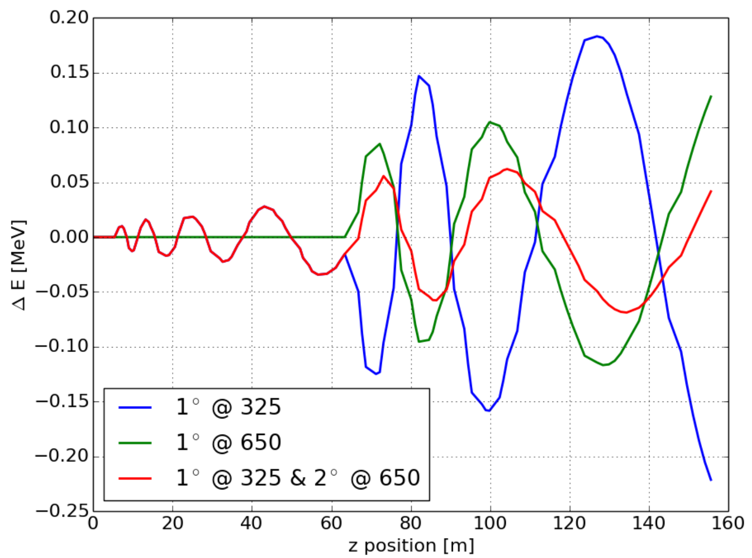

Linac output energy sensitivity to phase reference line phase errors at frequency transitions

J. Edelen

Fermilab

Simulating the impact of RF transients due to beam-loading on the beam-parameters

- The feedback model for the RF cavity was done in python (and compared with existing MATLAB models)
- The energy gain for each cavity was calculated using simulation results from PARMELA and TraceWin
- The phase advance during drift spaces was calculated using analytic models
- The beam current was assumed to be 2mA average during the pulse
- Left: Change in energy along the beam pulse due to uncompensated transients in the RF system
- Right: Change in phase along the beam pulse due to uncompensated transients in the RF system

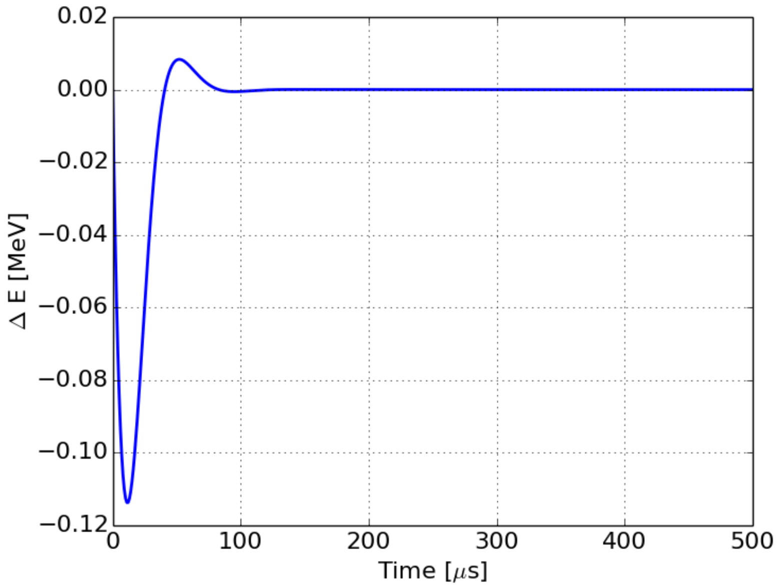

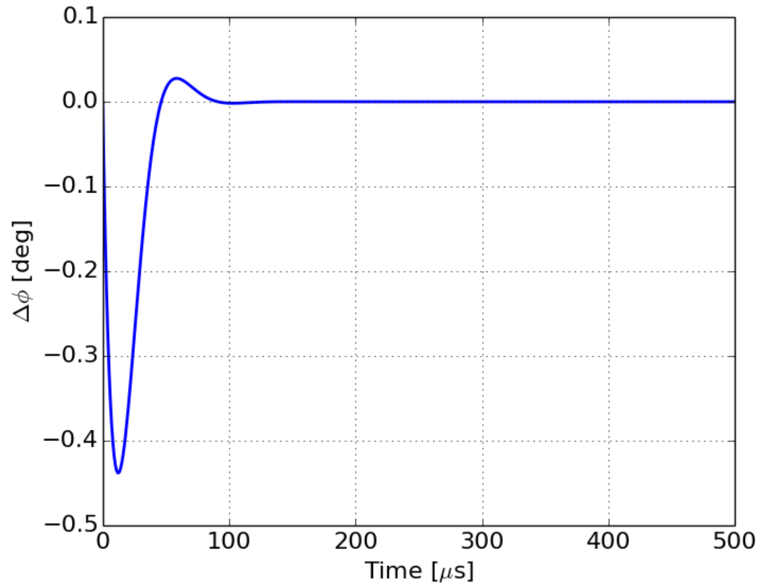

Simulating the impact of RF transients due to beam-loading on the beam-parameters

- We can analyze both the beam profile and individual slices along the LINAC
- Left: change in energy as a function of position along the LINAC for six different RF buckets along the beam pulse
- Right: Change in phase as a function of position along the LINAC or six different RF buckets along the beam pulse

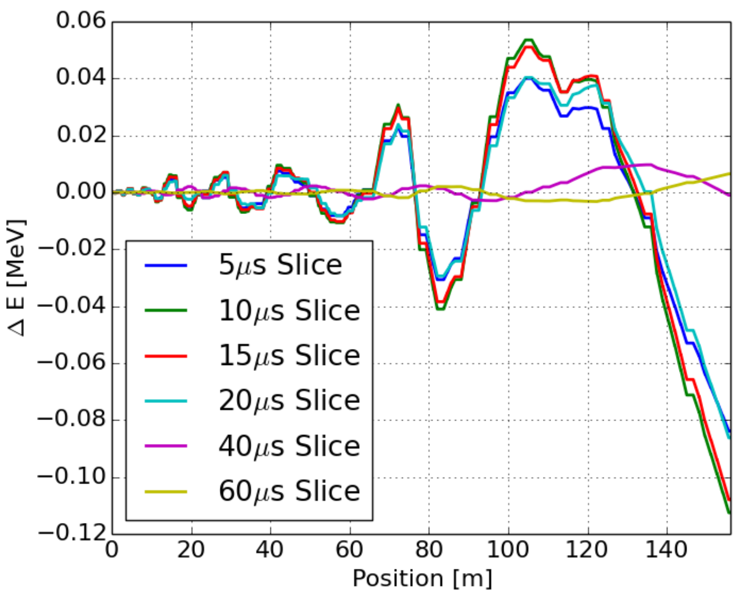

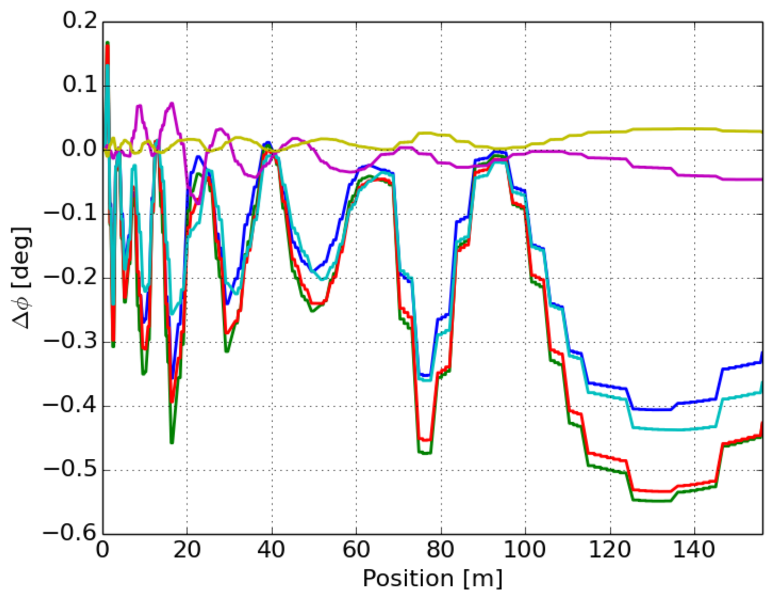

Cavity drive down to reduce cryogenic load

Pforward = 60 kW

Preverse = 230 kW

VSWR= -3.087922

Power coupler, waveguide and circulator:

-3x nominal forward Voltage

-5x power

Full drive down is not possible

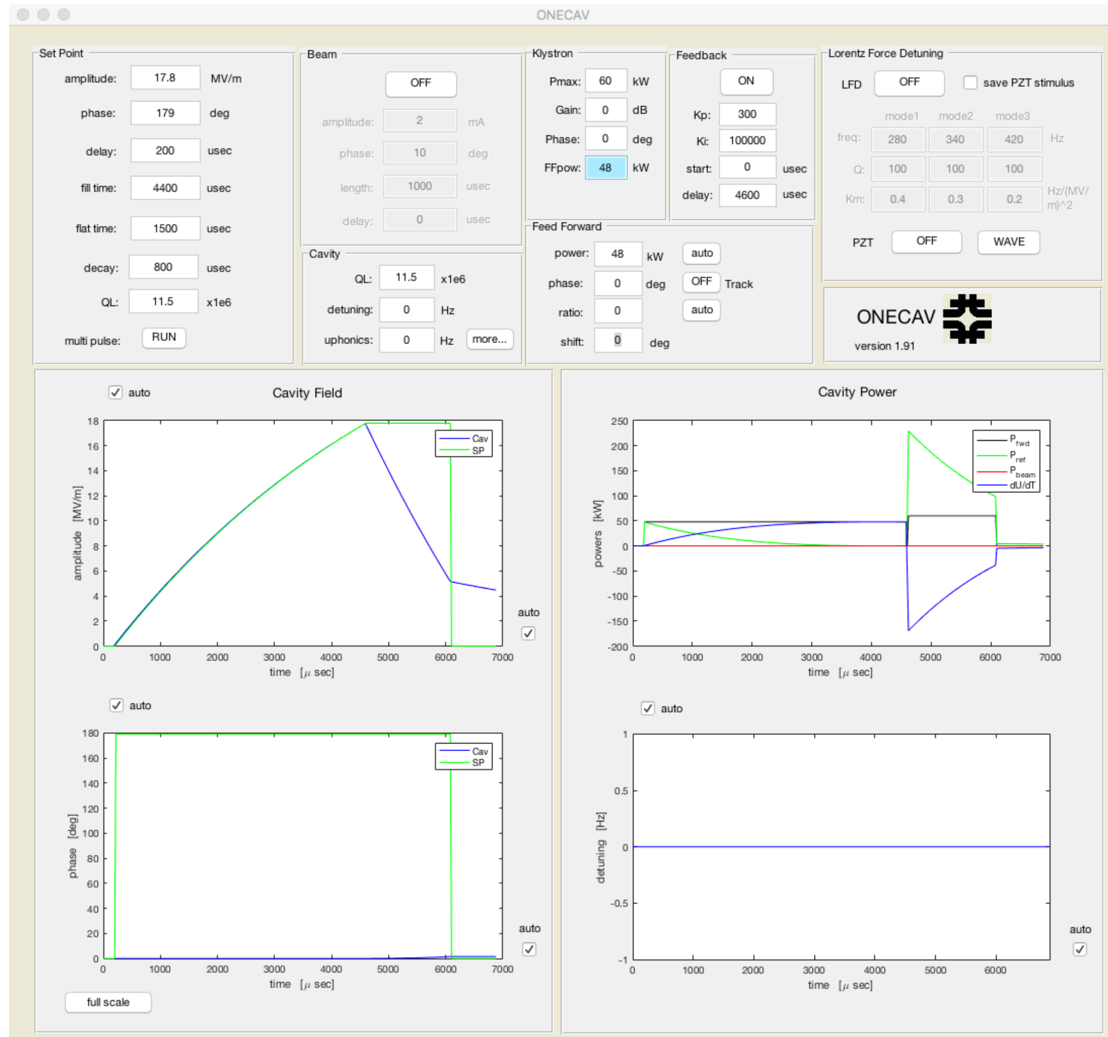

Fermilab PIP-II

Beam-based Phase Calibration

- In theory the average beam phase can be computed from cavity field due to beam-loading

$$\phi_{\mathrm{b}} = \tan^{-1}\left(\frac{\int_{t_0}^{t_1} V^{Q}_{\mathrm{cav-beam}}(t)dt}{\int_{t_0}^{t_1} V^{I}_{\mathrm{cav-beam}}(t)dt}\right)$$

- However this relies on proper background subtraction and some, albeit minor, assumptions about the profile of the beam
- First test is to try and reconstruct the phase of an ideal disturbance that is driven by the LLRF system
  - Some unexpected behavior is still under investigation
- Top: Integrated cavity voltage due to the ideal disturbance as a function of phase
- Bottom: Difference between reconstructed phase and drive phase as a function of the drive phase

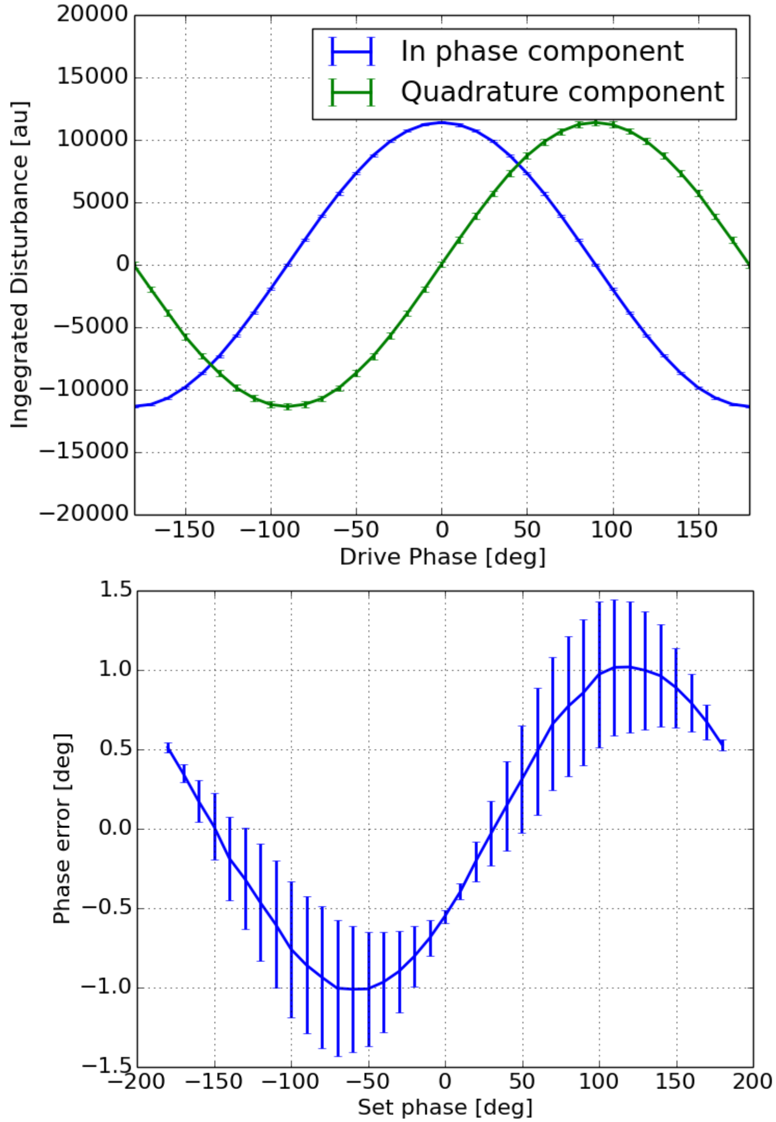

Beam-based Phase Calibration

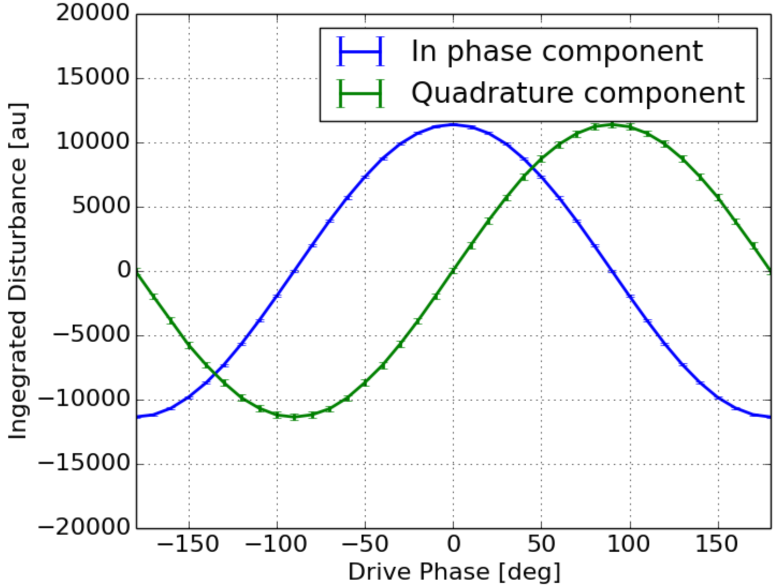

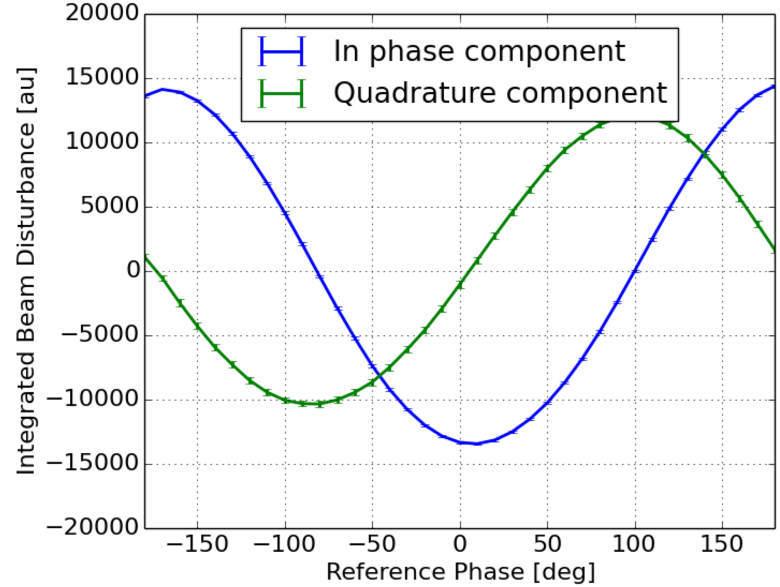

Integrated cavity field due to beam loading as a function of the drive phase for an ideal disturbance driven from the LLRF system

Integrated cavity field due to beam loading as a function of the drive phase for a 4.9mA beam in the PI-Test bunching cavity. Note the I and Q components are not symmetric.

J. Edelen

Environmental Considerations

Cooling

- Gallery temperature is not specified for tight regulation
  - This may require closed water cooled racks to meet RF stability requirements

Electrical service

- On mains power loss, cavities must be detuned to avoid mechanical distortion on warmup
- UPS power will be required to drive tuner stepper motors on all cavities.

Fermilab

RF Interlocks Overview
P. Prieto

RF Interlocks Objectives

- The primary objective of the RF Interlocks is to protect the SSA, Coupler, and Cavity from damage due to energy deposition during a fault condition.
- To achieve this goal the system must monitor signals such as SSA forward power, coupler forward and reflected power as well as cavity transmitted power.
- Additionally, signals such as coupler window temperature, presence of arcs in the coupler, field emission detection also are part of the interlocks system.
- The RF interlocks inhibits the LLRF to the SSA by opening a fast switch < 1 usec preventing RF power from feeding an arc.

RFPI Hardware Prototype at Meson Detector Building

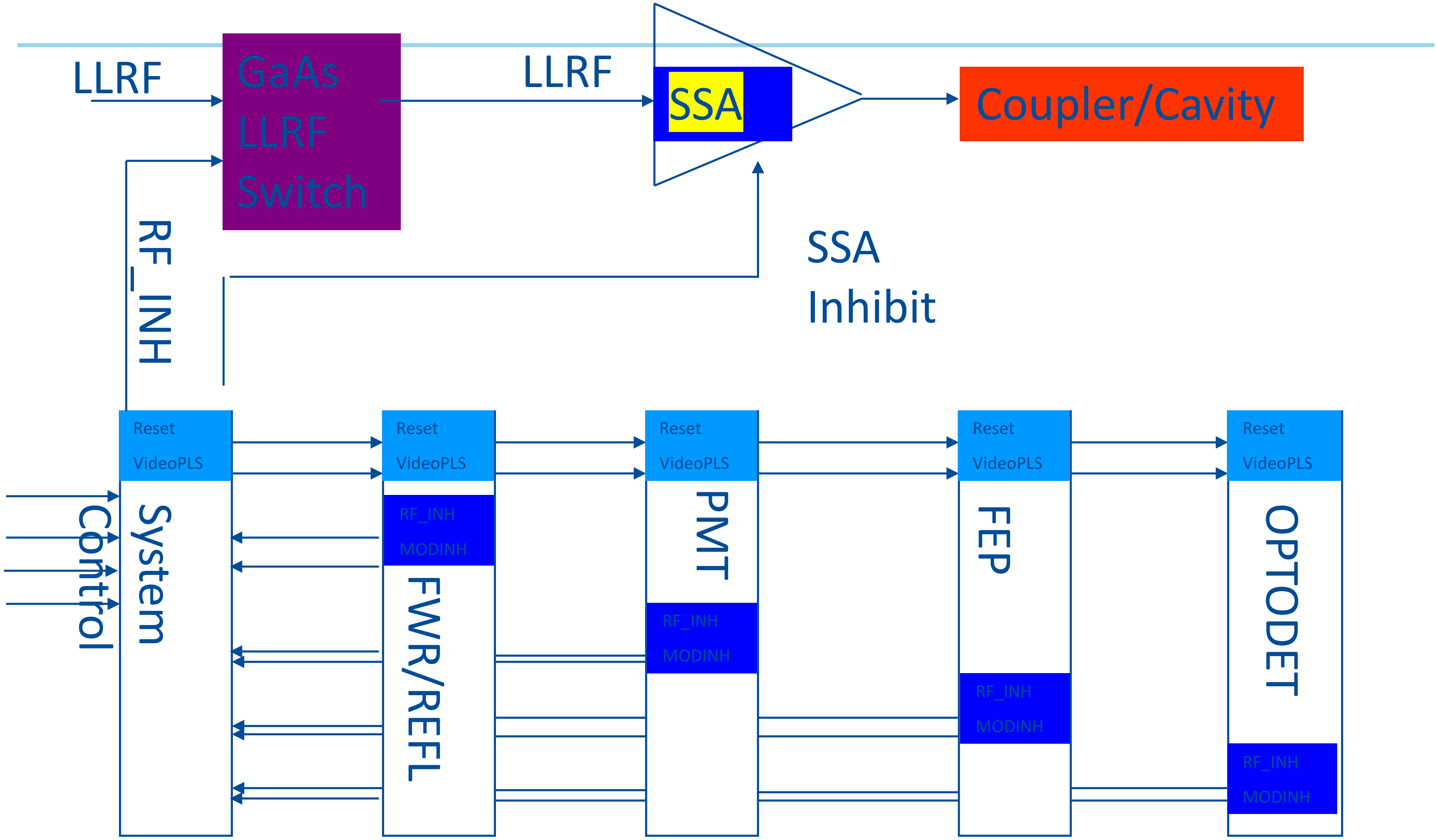
LLRF
GaAs
LLRF
Switch
LLRF
SSA
Coupler/Cavity
RF_INH
SSA
Inhibit
Reset
VideoPLS
System
Control
Reset
VideoPLS
RF_INH
MODINH
FWR/REFL
Reset
VideoPLS
PMT
RF_INH
MODINH
Reset
VideoPLS
FEP
RF_INH
MODINH
Reset
VideoPLS
OPTODET
RF_INH
MODINH

Conclusions

- The PIP-II LLRF design is an evolution of Fermilab designs and our collaboration efforts with LCLS-II
- IIFC joint designs in LLRF and RFPI are are making good progress and we are counting on their hardware and software contributions
- We will continue to gain operational experience at PIP2-IT and the various test stands with narrowband pulsed SRF cavities.

Thank you for your attention!

Backup slides

IIFC Deliverable Schedule

	Q1-16	Q2-16	Q3-16	Q4-16	Q1-17	Q2-17	Q3-17	Q4-17	Q1-18	Q2-18	Q3-18	Q4-18	Q1-19	Q2-19
RF Interlock														
Design and Certification 2 DAE	★ DAE													
Certification at FNAL				★ Fermilab										
RFPI for HTS2								★ DAE						
RFPI for SSR1											★ DAE			
RF Power system Ready for 1st SSR1 Cryomodule/HTS2												★ Fermilab		
RFPI for HB650													★ DAE	
LLRF System														
Initial Design of the System					★ Fermilab									
Prototype and Certification									★ DAE ★ Fermilab					
LLRF for HTS2										★ DAE				
LLRF for SSR1											★ DAE			
RF Power system Ready for 1st SSR1 Cryomodule/HTS2												★ Fermilab		
LLRF for HB650														★ DAE

★ Fermilab Milestone
★ DAE Milestone
+6 Months of schedule Contingency included in FY18 and 19 deliverables

A prototype RF protection and interlock has been delivered and tested at Fermilab

LLRF is on a reasonable pace for 2018 delivery

RFPI boards

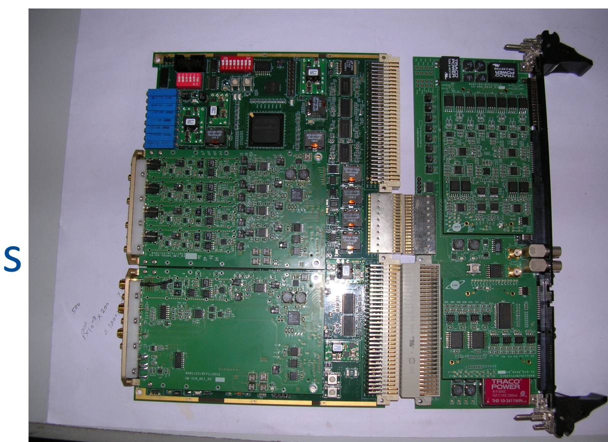

Brian Chase - Fermilab

Charge #1

- SPM – Low Level RF and RF Integration
- Started at Fermilab in 1982 and have work experience in cryogenics, power supplies, D0 detector electronics and beam Instrumentation
- LLRF – Linac, Main Injector, Tevatron, Recycler Ring
- SRF LLRF – Proton Driver, ILC, ILCTA, DESY (9mA Tests)
- LCLS-II, CMTS, PIP-II

- LLRF Team
  - AD LLRF - E. Cullerton, P. Varghese, J. Edelen, J. Einstein-Curtis, D. Klepec
  - IIFC - G. Joshi, S. Khole, D. Sharma, & many others
  - CSU – A. Edelen

System on Module Multi-cavity Field Controller (SOM-MFC)

SOM is socketed and upgradable

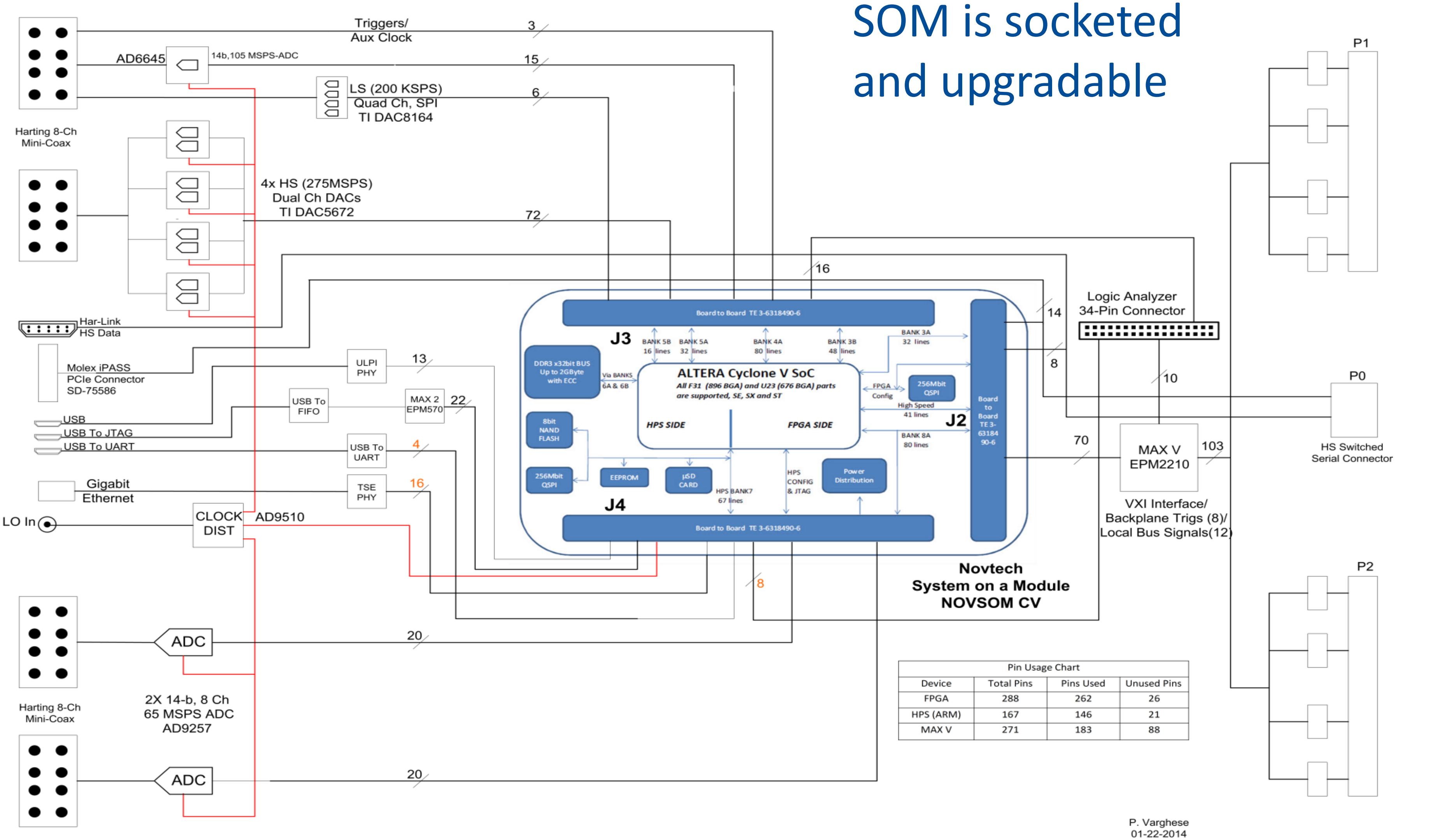

Pin Usage Chart			
Device	Total Pins	Pins Used	Unused Pins
FPGA	288	262	26
HPS (ARM)	167	146	21
MAX V	271	183	88

Fermilab PIP-II

System on Chip Multi-channel Field Controller

(16) 14 bit ADCs (8)14 bit DACs System on Module

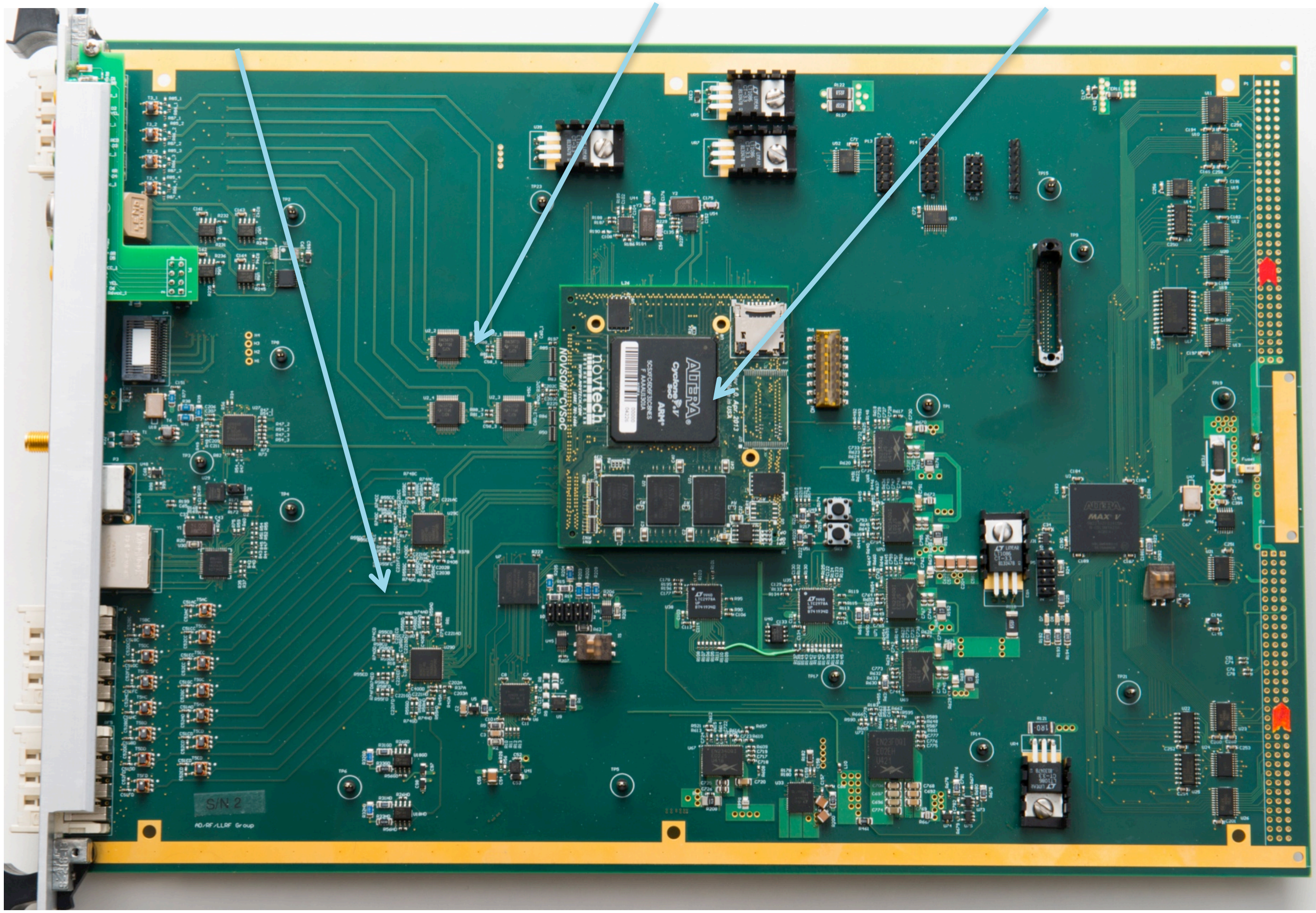

Dual core Arm processor with FPGA eliminates the need for a backplane and CPU card

PIP2-IT Low Level RF

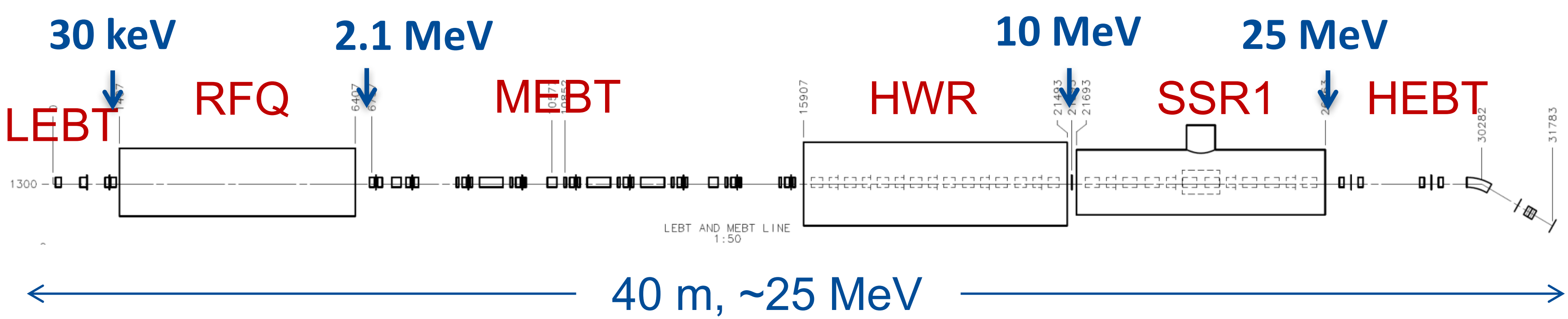

- Drive 20 accelerating structures
- 3 RF frequencies
- Master Oscillator and phase reference lines
- 0.01% amplitude and 0.01 deg. Phase regulation goal

Cavity RF operating parameters

#	Frequency (MHz)	Section	Amplitude (MV)	Synchronous Phase (deg)	Pg(kW)
1	162.5	MEBT	0.088	-90	2.67
2	162.5	MEBT	0.065	-90	1.45
3	162.5	MEBT	0.079	-90	2.13
4	162.5	HWR	0.44	-48.06	0.325
5	162.5	HWR	0.7	-35	0.789
6	162.5	HWR	0.85	-33.95	1.155
7	162.5	HWR	1	-26	1.618
8	162.5	HWR	1.5	-24.03	3.312
9	162.5	HWR	1.5	-20.02	3.351
10	162.5	HWR	1.6	-22	3.724
11	162.5	HWR	1.7	-23.98	4.105
12	325	SSR1	1	-32.96	0.904
13	325	SSR1	1	-29.99	0.946
14	325	SSR1	1.1	-28.01	1.127
15	325	SSR1	1.25	-27.03	1.399
16	325	SSR1	1.5	-26.03	1.89
17	325	SSR1	1.5	-27.01	1.915
18	325	SSR1	1.5	-25	1.956
19	325	SSR1	2.2	-23.98	3.622
20	243.75	HEBT	1.07*	n/a	2.9

Example of Microphonic Detuning at CMTS-1

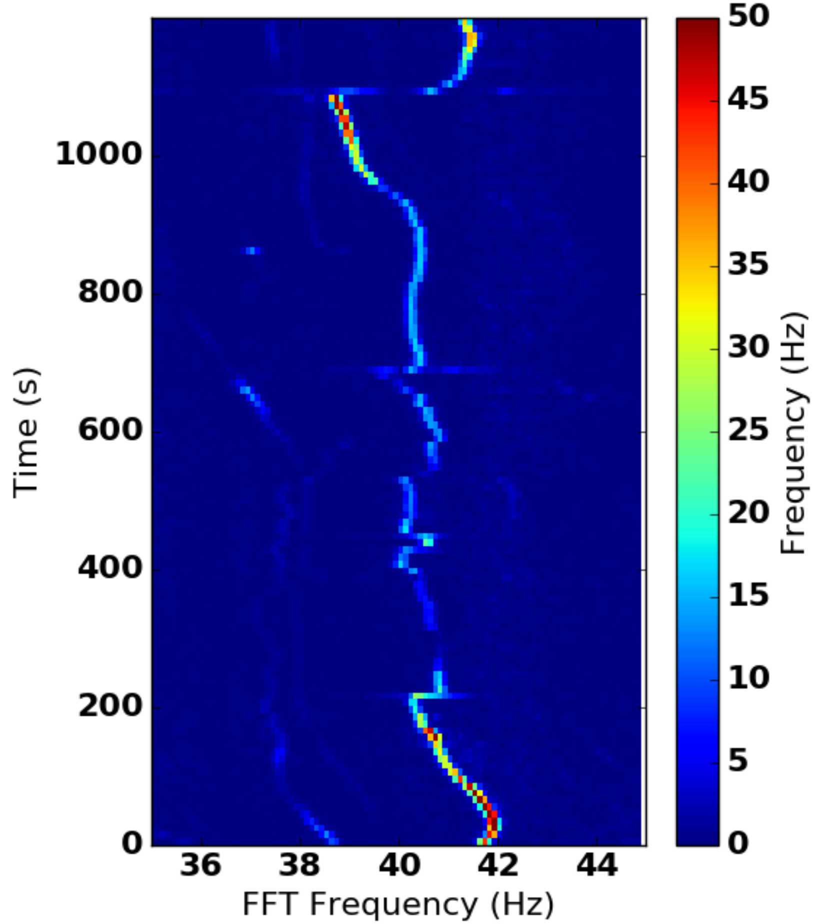

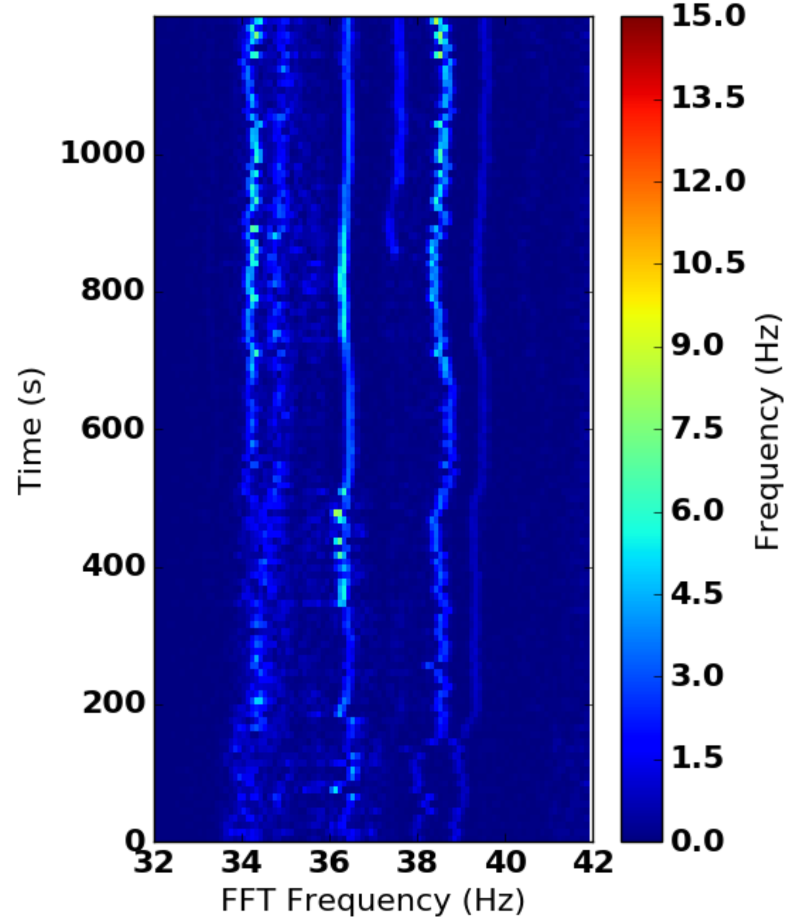

Main source is believed to be pressure fluctuation from a check valve in the helium return line and will be fixed in current shutdown. Resonance control is every system's responsibility.

RF Power budget and QI

Table 2.10: Requirements to RF power*

CM type	Power trans-ferred to beam per cav. (kW)	Microphonics amplitude (Hz)	Cavity half-bandwidth, $f/2Q_L$, (Hz)	Power transfer efficiency	Power margin	Peak RF power per cavity (kW)
HWR	4	20	33	90%	80%	6.5
SSR1	4.1	20	43	90%	80%	6.1
SSR2	10	20	28	90%	80%	17
LB 650	23.8	20	29	94%	80%	38
HB 650	39.8	20	29	94%	80%	64

* Powers are computed for beam current of 2 mA. Allowances for transmission loss and microphonics suppression are included for the peak RF power.

♦ Microphonics amplitude represents a target value for maximum cavity detuning due to microphonics.

Total cavity detuning budget including LFD

Measured LFD is 22 times larger than the entire resonance error budget

Table 2.11: Functional requirement specifications to cavity detuning due to helium pressure variations and Lorentz force detuning

CM type	HWR	SSR1	SSR2	LB650	HB650
Sensitivity to He pressure (FRS), df/dP, Hz/Torr	<25	<25	<25	<25	<25
… (measurements), df/dP, Hz/Torr	13	4.0	-	-	-
Estimated LFD sensitivity, df/dE^2, Hz/(MV/m)^2	-	-5.0	-	-0.8	-0.5
… (measurements), df/dE^2, Hz/(MV/m)^2	-1.5♦	-4.4	-	-	-
Estimated LFD at nominal voltage (FRS), Hz	-	-500	-	-192	-136
… (measurements) at nominal voltage, Hz	-122.4	-440	-	-	-

May need real-time feedback during pulse

Ongoing cavity design efforts to lower these numbers

RFQ Resonance control status

- Currently meeting specification
  - Specification was to recover the RFQ in less than 10 times the RF recovery time
  - Goal of less than twice the RF recovery time
  - We anticipate meeting our goal requirement after the next round of improvements
- The controller interfaces with the water instrumentation, ACNET, and LLRF
- The controller framework is modular and can easily be improved or adapted to new systems
- Plans to improve performance will decrease the initial start time and decrease the trip recovery time

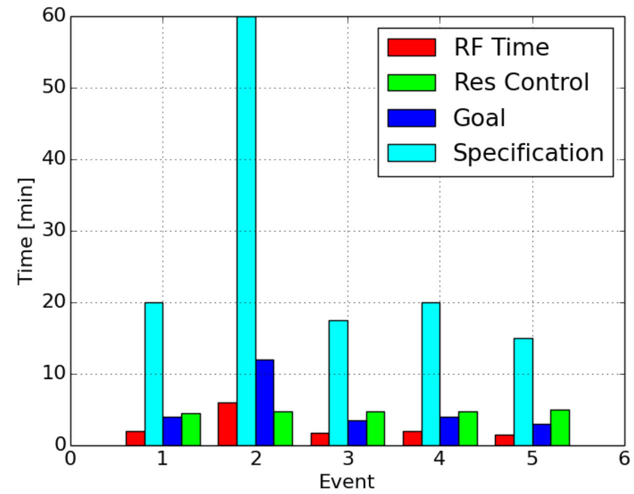

Vane voltage: Red
Frequency error: Blue
Grey: RFQ ramp, resonance control is idle, LLRF is in SEL
Orange: Resonance control bringing RFQ to frequency, LLRF is in SEL
Green: RFQ is in GDR and LLRF feedback is active

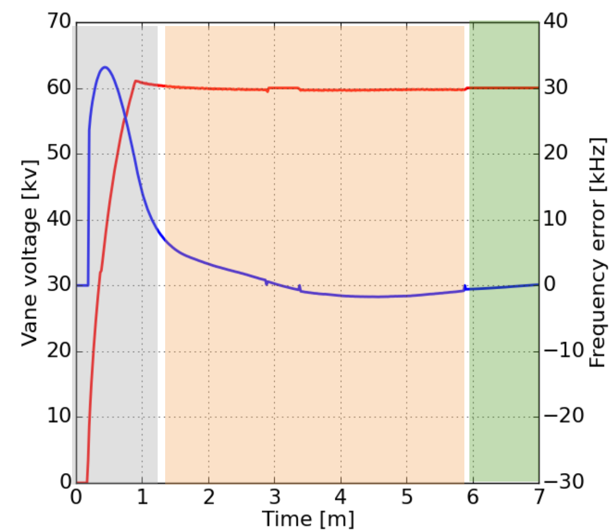

Table 2.6: General parameters of SC cryomodules

CM type	Cavities per CM	Number of CMs	CM configuration•	CM length (m)	Q_0 at 2K (10^{10})	Surface resistance, (nΩ)	Loaded Q (10^6)
HWR	8	1	8 × (sc)	5.93	0.5	9.6 (2.75♠)	2.7
SSR1	8	2	4 × (csc)	5.2	0.6	14 (10#)	3.7
SSR2	5	7	sccsccsc	6.5♦	0.8	14.4	5.8
LB650	3	11	ccc	3.9♦	2.15	8.9	11.3
HB650	6	4	cccccc	9.5♦	3	8.7	11.5

• Within the cryomodule (CM) configuration column "c" refers to an individual accelerating cavity, and "s" to a focusing solenoid.

♦ This number represents the present estimate of the cryomodule lengths. It will be finalized with advances in the cryomodule design.

♠ Measured value based on recent measurements of two HWR cavities at 2 MV accelerating voltage.

Based on recent measurements of SSR1 cavities made of CABOT niobium. We expect to get better results for the SSR2 cavities to be made of material, which satisfies Fermilab specifications [19].

Table 2.5: Main electro-dynamical parameters of SC cavities

Cavity type	Aperture (diameter) (mm)	Effective length (cm)	Accelerating gradient * (MV/m)	E_{peak} * (MV/m)	B_{peak} * (mT)	$(R/Q)^5$ (Ω)	G (Ω)
HWR	33	20.7	9.7	44.9	48.3	272	48
SSR1	30	20.5	10	38.4	58.1	242	84
SSR2	40	43.8	11.4	40	64.5	297	115
LB650	83	74.6	15.9	39.4	74.6	356	187
HB650	118	112.0	17.8	38.9	73.1	610	260

* For energy gain per cavity presented in Table 2.4 where the cavity effective length was computed as $L_{eff}=c\beta_{opt}n_{cell}/2f$.

Fermilab PIP-II

5 min ramp. Mostly automated (operator tuning at 14 minutes to speed things up a little)

Testing faster start, not fully automated. Kink in resonance frequency at 14 minutes was due to operator tuning not automatic tuning.

Vane voltage: Red
Frequency error: Blue
Grey: RFQ ramp, resonance control is idle, LLRF is in SEL
Orange: Resonance control bringing RFQ to frequency, LLRF is in SEL
Green: RFQ is in GDR and LLRF feedback is active

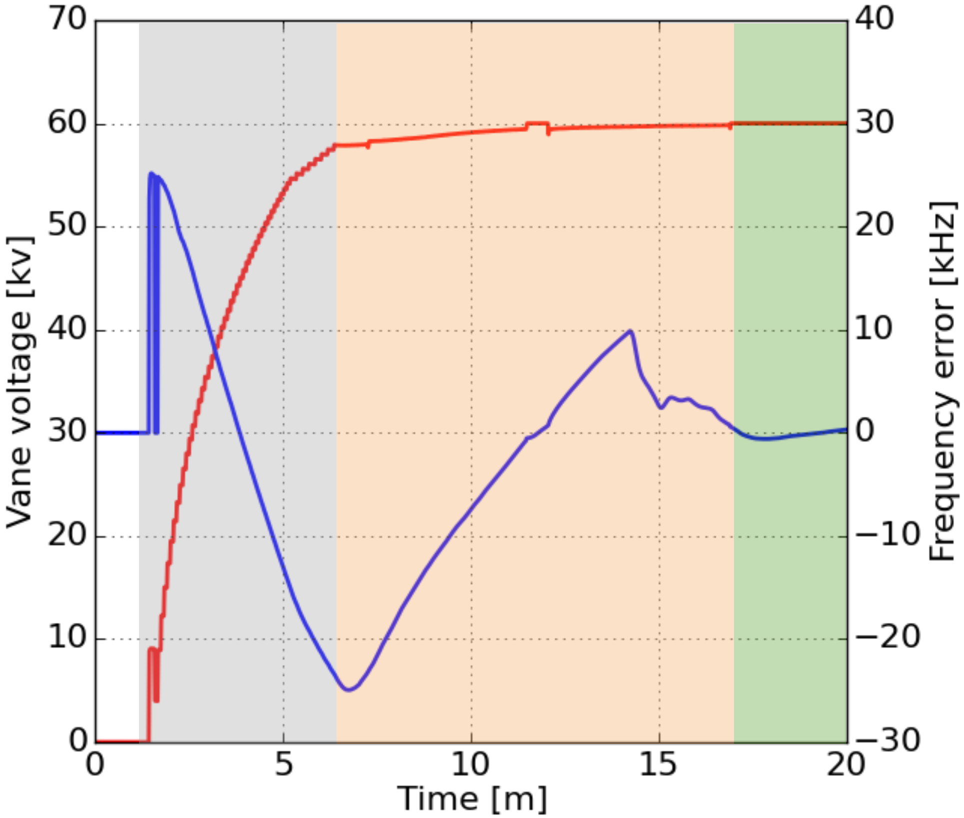

Fermilab PIP-II

Baseband cavity and controller model

- Baseband cavity model is a low pass filter with a bandwidth determined by Q_l and ω_0: $T_{cav}(s) = \frac{\omega_0/Q_l}{s+\omega_0/Q_l}$
- In the simplest case the feed-forward component of the system is simply the set-point
- Initially assume that the I and Q loops are driven with the same PI parameters

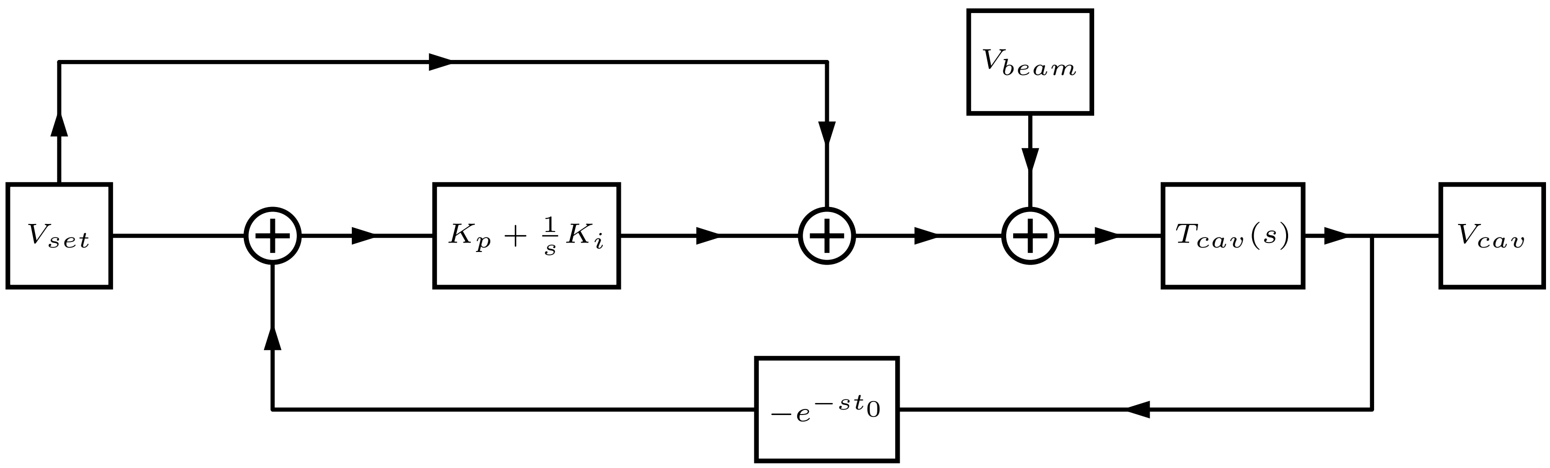

Figure: Baseband model of LLRF control system. Middle row (from left to right): Set-point, summing junction for feedback, PI controller, summing junction for feed-forward, summing junction for beam-loading, cavity transfer function, and cavity probe signal. Bottom row: group delay (negative for negative feedback). Top row: beam-loading

RFQ vane system step response

	initial	transient	steady state
Time	0	7.2 min	115.4 min
Δf_{res}	0	46.13 kHz	21.15 kHz
TT_{101}	22.280 ^{o}C	25.796 ^{o}C	25.649 ^{o}C
TT_{102}	31.489 ^{o}C	28.126 ^{o}C	26.141 ^{o}C
TT_{103}	30.941 ^{o}C	27.639 ^{o}C	26.284 ^{o}C

flow path	time delay [s]
$TT_{101} \rightarrow TT_{103}$	1.0
$TT_{103} \rightarrow TT_{102}$	17.0

- Transient response of the RFQ resonant frequency due to change in the vane flow control valve. Prior to changing the flow valve, the intermediate skid was cooled to approximately 25C. The control valve was stepped from 0% open to 50% open.